Twenty-first Century Drought Projections in the CMIP6 Forcing Scenarios

B. I. Cook[1,2], J. S. Mankin[2,3], K. Marvel[1,4], A. P. Williams[2], J. E. Smerdon[2], K. J. Anchukaitis[2,5,6,7]

[1]NASA Goddard Institute for Space Studies, New York, New York, USA
[2]Lamont-Doherty Earth Observatory, Columbia University, Palisades, New York, USA
[3]Department of Geography, Dartmouth College, Hanover, New Hampshire, USA
[4]Department of Applied Physics and Applied Mathematics, Columbia University, New York, NY, USA
[5]School of Geography and Development, University of Arizona, Tucson, AZ, USA
[6]Laboratory of Tree-Ring Research, University of Arizona, Tucson, AZ, USA
[7]Department of Geosciences, University of Arizona, Tucson, AZ, USA

Key Points:

- The sign and magnitude of drought responses in the CMIP6 projections depend on the region, season, and drought metric being analyzed
- Soil moisture and runoff drying is more widespread and robust than precipitation, with the severity increasing strongly with warming
- The sign of CMIP6 responses aligns with previous results from CMIP5, suggesting similar physical processes and underlying uncertainties

Corresponding author: Benjamin I Cook, `benjamin.i.cook@nasa.gov`

This article has been accepted for publication and undergone full peer review but has not been through the copyediting, typesetting, pagination and proofreading process, which may lead to differences between this version and the Version of Record. Please cite this article as doi: 10.1029/2019EF001461

Abstract

There is strong evidence climate change will increase drought risk and severity, but these conclusions depend on the regions, seasons, and drought metrics being considered. We analyze changes in drought across the hydrologic cycle (precipitation, soil moisture, and runoff) in projections from Phase Six of the Coupled Model Intercomparison Project (CMIP6). The multi-model ensemble shows robust drying in the mean state across many regions and metrics by the end of the 21st century, even following the more aggressive mitigation pathways (SSP1-2.6 and SSP2-4.5). Regional hotspots with strong drying include western North America, Central America, Europe and the Mediterranean, the Amazon, southern Africa, China, Southeast Asia, and Australia. Compared to SSP3-7.0 and SSP5-8.5, however, the severity of drying in the lower warming scenarios is substantially reduced and further precipitation declines in many regions are avoided. Along with drying in the mean state, the risk of the historically most extreme drought events also increases with warming, by 200–300% in some regions. Soil moisture and runoff drying in CMIP6 is more robust, spatially extensive, and severe than precipitation, indicating an important role for other temperature-sensitive drought processes, including evapotranspiration and snow. Given the similarity in drought responses between CMIP5 and CMIP6, we speculate both generations of models are subject to similar uncertainties, including vegetation processes, model representations of precipitation, and the degree to which model responses to warming are consistent with observations. These topics should be further explored to evaluate whether CMIP6 models offer reasons to have increased confidence in drought projections.

Plain Language Summary

Drought is an important natural hazard in many regions around the world, and there are significant concerns that climate change will increase the frequency or severity of drought events in the future. Compared to a world before anthropogenic climate change, the latest state-of-the-art climate model projections from CMIP6 show robust drying and increases in extreme drought occurrence across many regions by the end of the 21st century, including western North America, Central America, Europe and the Mediterranean, the Amazon, southern Africa, China, Southeast Asia, and Australia. While these changes occur even under the most aggressive climate mitigation pathways, the models show substantial increases in the extent and severity of this drying under higher warming levels, highlighting the value of mitigation for reducing drought-based climate change impacts. Given the significant response to even modest warming, however, and evidence that climate change has already increased drought risk and severity in some regions, adaptation to a new, drier baseline will likely be required even under the most optimistic scenarios.

1 Introduction

Shifts in hydroclimate, especially drought, are some of the most important regional consequences of climate change for people and ecosystems (Breshears et al., 2018; Gosling & Arnell, 2016; Humphrey et al., 2018; Vicente-Serrano et al., 2019). Analyses of climate model experiments are especially useful for evaluating how climate change affects drought, including multi-model efforts such as those organized as part of the Fifth Phase of the Coupled Model Intercomparison Project (CMIP5) (Taylor et al., 2012). Studies using CMIP5 simulations have advanced our understanding of regionally heterogeneous hydroclimate responses to warming (Cook et al., 2014; Dai, 2013; Hessl et al., 2018), highlighted areas where increases in drought risk and severity will be especially pronounced (Cook et al., 2015; Seager et al., 2019), investigated mechanisms that may explain why different drought variables respond differently to warming (A. Berg et al., 2017; Lemordant et al., 2018; Mankin et al., 2019; Milly & Dunne, 2016; Swann et al., 2016), and quantified the detection and attribution of climate change signals in observed hydroclimate trends and drought events (Kelley et al., 2015; Marvel et al., 2019; Williams et al., 2015).

Analyses of the CMIP5 simulations have revealed an array of drought responses showing strong and consistent agreement across models in response to anthropogenic forcing, while also highlighting important, and sometimes irreducible, uncertainties (Cook et al., 2018; Knutti & Sedlacek, 2013; Mankin, Smerdon, et al., 2017; Mankin, Viviroli, et al., 2017). Precipitation responses to climate change, for example, are highly uncertain for many regions and seasons (Knutti & Sedlacek, 2013), especially over land where the classic "wet-get-wetter/dry-get-drier" expectations do not hold (Byrne & O'Gorman, 2015; Greve et al., 2014; Held & Soden, 2006). This contrasts sharply with soil moisture and runoff, which generally show much more intense and widespread drying patterns (A. Berg et al., 2017; Cook et al., 2018), in part because of warming-induced increases in evaporative demand and total vegetation water use (Dai et al., 2018; Mankin et al., 2019). At the same time, plant physiological responses to rising atmospheric CO_2 concentrations also increase plant water use efficiency in models (Swann et al., 2016), potentially modulating surface drying while also emphasizing the important, but often complex and uncertain, role of vegetation processes (Lemordant et al., 2018; Trugman et al., 2018). Even in cases where models may strongly agree on the sign and magnitude of the drought response, however, overreliance on consistency as a metric to guide model interpretations may lead to over-confidence if the strong multi-model agreement arises from systematic errors across models (Tierney et al., 2015). Thus, while the CMIP5 projections provide some of the most comprehensive information on how drought will respond to climate change, it is important to reassess the state of knowledge as new datasets and research tools become available.

Recently, new simulations from the latest, state-of-the-art climate models participating in Phase Six of the Coupled Model Intercomparison Project (CMIP6) have become available (Eyring et al., 2016). This provides a new opportunity to analyze hydroclimate and drought responses to climate change in the projections and revisit conclusions from previous community modeling efforts. Using a multi-model ensemble (MME) drawn from CMIP6, we investigate changes in precipitation, soil moisture, and runoff across a range of 21^{st}-century development and radiative forcing scenarios (Shared Socioeconomic Pathways; SSPs) developed for ScenarioMIP (O'Neill et al., 2016). We focus our analyses around three primary research questions: (1) How do changes in drought risk and severity compare across different CMIP6 forcing scenarios?; (2) How different is the extent and intensity of changes in meteorological (precipitation) drought versus agricultural (soil moisture) and hydrological (runoff) drought?; and (3) How do results from CMIP6 compare to those from CMIP5?

2 Materials and Methods

2.1 CMIP6 Multi-Model Ensemble

We downloaded diagnostic output from climate models in the CMIP6 database (`https://esgf-node.llnl.gov/search/cmip6/`), using the "historical" (1850–2014) simulations conducted as part of the core DECK experiments (Eyring et al., 2016) and four SSPs (2015–2100) from ScenarioMIP (O'Neill et al., 2016). The historical simulations are forced with estimates of natural (e.g., volcanic eruptions, solar and orbital variability) and anthropogenic (e.g., greenhouse gas emissions, aerosols, land use change) climate forcings, with the goal of simulating climate change and variability over the time period covered by the observational record. The SSPs represent a range of future greenhouse gas emission and land use change scenarios estimated from integrated assessment models and based on various assumptions regarding economic growth, climate mitigation efforts, and global governance. Using these assumptions, the SSPs are used to generate different radiative forcing pathways, and associated warming, out to the end of the 21^{st} century. To consider a range of possible futures, we use simulations from four SSPs, drawn from Tier

Table 1. The number of ensemble members from each model and SSP scenario used to construct the multi-model CMIP6 ensemble, along with each model's equilibrium climate sensitivity (ECS; K/2xCO_2) and reference for submission to CMIP6. ECS values taken from Pendergrass (2019) and `https://www.carbonbrief.org/cmip6-the-next-generation-of-climate-models-explained`.

	Ensemble Members					
Model	SSP1-2.6	SSP2-4.5	SSP3-7.0	SSP5-8.5	ECS	Reference
BCC-CSM2-MR	1	1	1	1	3.1	Wu et al. (2018)
CanESM5	9	9	9	9	5.6	Swart et al. (2019)
CESM2	1	1	2	2	5.2	Danabasoglu (2019a)
CESM2-WACCM	1	1	1	1	4.7	Danabasoglu (2019b)
CNRM-CM6-1	6	6	6	6	4.8	Voldoire (2018)
CNRM-ESM2-1	5	5	5	5	4.8	Seferian (2018)
GFDL-CM4	**NA**	1	**NA**	1	3.9	Guo et al. (2018)
GFDL-ESM4	1	1	1	**NA**	2.7	Krasting et al. (2018)
IPSL-CM6A-LR	3	2	10	1	4.5	Boucher et al. (2018)
MIROC-ES2L	1	1	1	1	2.7	Tachiiri et al. (2019)
MIROC6	3	3	3	3	2.6	Tatebe and Watanabe (2018)
MRI-ESM2-0	1	1	1	1	3.2	Yukimoto et al. (2019)
UKESM1-0-LL	5	5	5	4	5.3	Good et al. (2019)

1 of ScenarioMIP: SSP1-2.6 (+2.6 W m^{-2} imbalance; low forcing sustainability pathway), SSP2-4.5 (+4.5 W m^{-2}; medium forcing middle-of-the-road pathway), SSP3-7.0 (+7.0 W m^{-2}; medium- to high-end forcing pathway), and SSP5-8.5 (+8.5 W m^{-2}; high-end forcing pathway).

We selected specific models and ensemble members (listed in Table 1) that provided the following diagnostics from continuous (1850–2100) historical+SSP simulations: tas (2-m near surface air temperature; K), pr (precipitation rate, all phases; mm day^{-1}), mrsos (surface, top 10 cm, soil moisture content, all phases; kg m^{-2}), mrso (total soil moisture content, all phases summed over all layers; kg m^{-2}), mrros (total surface runoff leaving the land portion of the grid cell, excluding drainage through the base of the soil model; mm day^{-1}), and mrro (total runoff, including drainage through the base of the soil model; mm day^{-1}). These variables cover the full range of traditional physical drought categories: meteorological (precipitation), agricultural (soil moisture), and hydrological (runoff). The simulations represent an "ensemble of opportunity", constrained by the requirement that each simulation must provide all of the variables outlined above. While not all models provided theses variables for all SSPs, 11 of the 13 models are represented in each of the 4 SSPs, and 8 of these models have a consistent number of ensemble members across all four SSPs.

2.2 Analyses

For most analyses, we calculate anomalies and changes for the end of the 21st century, 2071–2100, relative to a baseline climatology of 1851–1880. This baseline is most representative of pre-industrial conditions in the historical simulations, allowing us to evaluate the full-scale of changes in climate and drought resulting from anthropogenic forcing. To test the sensitivity of our conclusions to our choice of baseline, and assess the potential for greenhouse gas mitigation to reduce future drought responses, we also evaluate end of 21st century changes relative to a more modern baseline representing the last 30 years of the historical simulations, 1985–2014. To improve legibility of the figures showing changes in individual seasons, which have a large number of subplots, the most extreme warming scenario (SSP5-8.5) is omitted from these figures.

Drought responses to warming can be highly seasonally dependent, so all analyses are conducted separately for different seasonal composites. For precipitation, we break the analysis into four 3-month seasons: December–February (DJF), March–May (MAM), June–August (JJA), and September–November (SON). For all the soil moisture and runoff fields, we use six-month averages: April–September (AMJJAS) and October–March (ONDJFM). To facilitate comparisons across models, all models are linearly interpolated to a new uniform 1.5° spatial resolution. When constructing the MME, all individual ensemble members within each model are averaged together first, and then the MME average is calculated across models to ensure that each model is weighted equally. Ensemble average changes are expressed in units of either percent change (precipitation, surface runoff, and total runoff) or standardized z-scores (surface soil moisture and total column soil moisture), calculated by subtracting the mean and dividing by the standard deviation of the time series from the baseline period. Z-scores are used for soil moisture variables that represent large pools of moisture, where significant changes may be small on a percentage basis, but still represent large changes relative to natural variability. All other calculations (e.g., robustness, changes in return frequency) are applied to the variables in their native units.

The relative agreement across models in the ensemble is assessed using the robustness metric R, described in detail in Knutti and Sedlacek (2013). This robustness indicator incorporates information on the magnitude and sign of the MME change, variability within each simulation, and the spread across models in the MME. A value of $R = 1.0$ indicates perfect agreement across models. A higher model spread or smaller signal will decrease R, while R will increase if the shape of the distribution or variability changes between time periods, even if the MME mean does not change. For our analyses, we use a threshold of $R \geq 0.90$ to determine whether our MME responses are robust, representing an intermediary value between the $R = 0.80$ ("good agreement") and $R = 0.95$ ("very good agreement") thresholds used by Knutti and Sedlacek (2013).

We also calculate changes in the risk, or likelihood of occurrence, of extreme single-year drought events. Extreme single-year droughts are defined as years with values, for any variable, equal to or below the 10$^{\text{th}}$ percentile of all years during the 1851–1880 baseline. We then calculate the percentile of equivalent or drier extreme drought events for 2071–2100, and use this information to determine the relative change in risk of these droughts. To avoid distorting or damping variability because of averaging across simulations, these drought frequency calculations are conducted at each grid cell for each variable and season by pooling all years from all available models and ensemble members together (results are similar if only one ensemble member from each model is used).

3 Results and Discussion

3.1 Warming Across the SSP Scenarios

All four SSP scenarios show strong warming over the full period of simulation from 1850–2100 (Figure 1; left panel). Temperature trajectories across the SSPs diverge most strongly after 2050, as emissions begin to slow or plateau in the more aggressive mitigation scenarios, SSP1-2.6 and SSP2-4.5. For 2071–2100, median warming (Figure 1, right panel) across the ensemble for each SSP is: +2.1 K (SSP1-2.6), +3.0 K (SSP2-4.5), +3.9 K (SSP3-7.0), and +4.9 K (SSP5-8.5). Even within each SSP, however, the spread in warming across models can be large (black dots, right panel in Figure 1), resulting in some significant overlap between adjacent scenarios, especially SSP3-7.0 and SSP5-8.5.

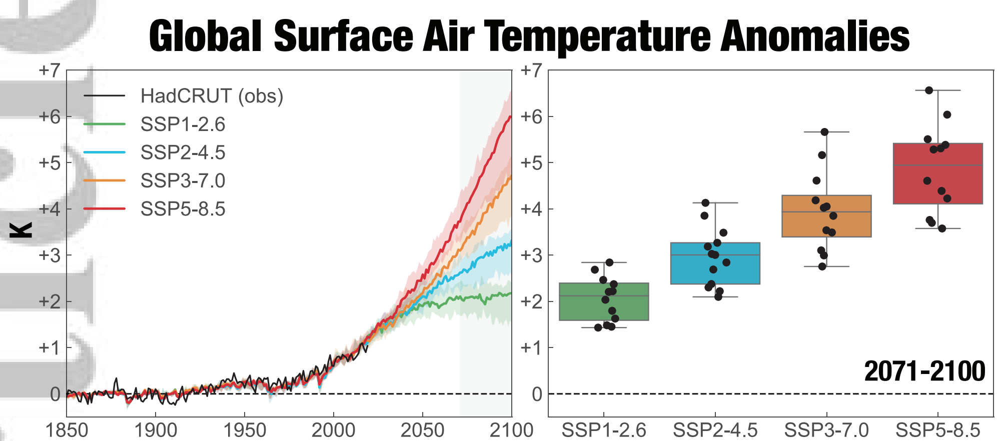

Figure 1. Global, annual average surface air temperature (SAT) anomalies (baseline 1851–1880) for the four SSP scenarios in our CMIP6 ensemble. Left panel: ensemble time series, showing the ensemble median (solid lines) and the interquartile range calculated across models (colored shading). Anomalies from observations in an updated version of the HadCRUT (version 4) global temperature dataset (Morice et al., 2012) are shown in black, using the same 1851–1880 baseline. Light grey shading is 2071–2100, the time interval used for construction of the box and jitter plots. Right panel: box and jitter plots for all models (median SAT anomaly, 2071–2100) in each SSP scenario. Individual model values are indicated by the black dots.

3.2 Precipitation

Increases in precipitation are widespread and robust across large land areas of North America, Asia, northern and eastern Africa, and the Middle East (Figure 2). During boreal winter (DJF) and spring (MAM), the largest anomalies occur across the mid- and high-latitudes of the Northern Hemisphere. This robust response is consistent with the precipitation response in the CMIP5 models (Knutti & Sedlacek, 2013), likely occurring as a consequence of increased atmospheric humidity in regions and seasons of mean moisture convergence, rising motion, and storm track activity. Similarly, precipitation also increases in extra-tropical South America east of the Andes Mountains and also major monsoon regions around the world, including West Africa, India, and Southeast Asia. Increases in monsoon regions are likely indicative of a warming-induced intensification of the monsoons in the mid- to late- wet season (e.g., SON in Southeast Asia), a pattern also previously documented in CMIP5 (Lee & Wang, 2014; Seth et al., 2013).

By contrast, drying patterns in precipitation are not as robust and are much more localized. The largest declines occur in Mediterranean-type climate regions, including the Mediterranean, southwest Australia, and along the western coasts of South America and southern Africa, in line with observations and analyses of previous generations of climate models (Hoerling et al., 2012; Seager et al., 2019). Declines also occur during the early part of the rainy season in many monsoon regions (e.g., MAM in Southeast Asia), indicative of delayed monsoon onset also shown in CMIP5 models (Lee & Wang, 2014; Seth et al., 2013). Other regions where widespread drying occurs include Central and Northern Europe (JJA), Central America (all seasons except SON), the Amazon (all seasons, intensified during JJA and SON), southern Africa (all seasons, intensified during JJA and SON), and southeast Australia (JJA and SON). Over the western United States, the main precipitation declines occur over the southwest in spring (MAM) (Ting et al., 2018) and the Pacific Northwest in summer (JJA).

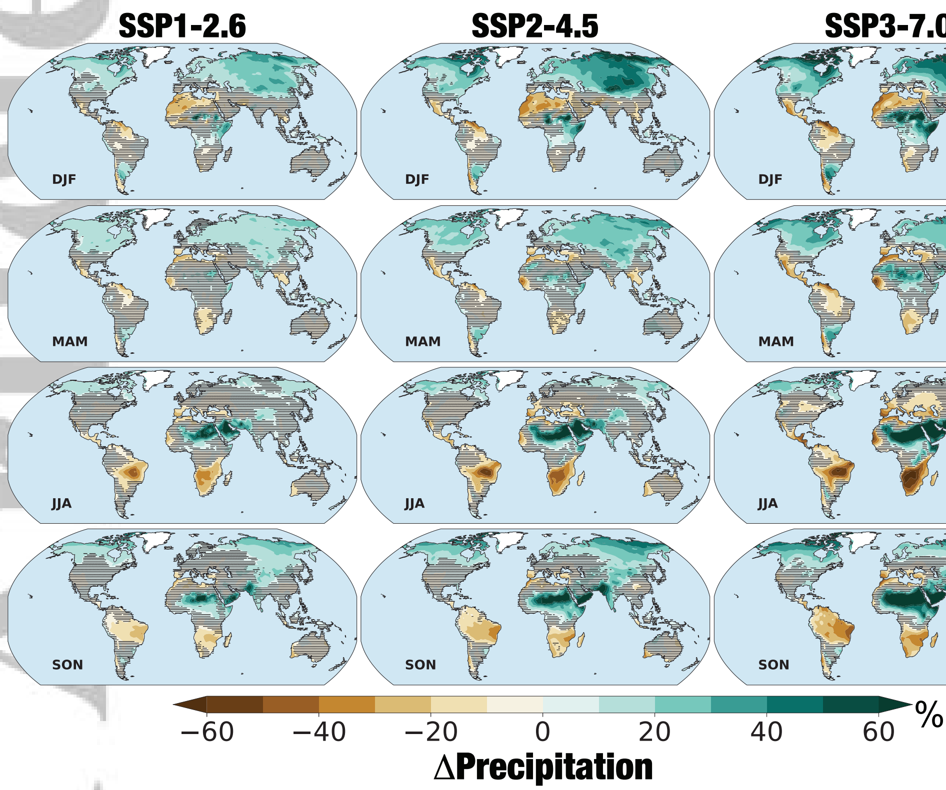

Figure 2. Three-month seasonal average total precipitation changes (% change, 2071-2100 versus 1851–1880) in the multi-model ensemble mean in the SSPs. Areas where changes are non-robust (R<0.90) are indicated by hatching.

3.3 Soil Moisture

Surface soil moisture drying (Figure 3, top panels) is more robust and widespread compared to precipitation, especially over North America, Europe and the Mediterranean, South America outside of Argentina, southern Africa, and in southwestern and southeastern Australia. Notably, this drying extends into regions where precipitation is increasing or where changes in precipitation are non-robust, including northern and eastern Europe and the Central Plains in North America. This highlights the importance of other processes that can reallocate moisture away from the surface towards evapotranspiration, including increased evaporative demand in the atmosphere (Dai et al., 2018) and greater vegetation water use (Mankin et al., 2019). The impact of even the most conservative warming scenarios is apparent in the soil moisture changes, where, under SSP1-2.6, much of western North America and Europe still experience a one to two standard deviation shift towards drier mean conditions, especially during the warm season (AMJJAS). The few regions where robust surface soil moisture increases occur are mostly aligned with areas where the strongest precipitation increases are projected, including East Africa, Central Asia, Argentina, and and monsoonal regions of West Africa and India.

Drying in the total column soil moisture is also more widespread (Figure 3, bottom panels) compared to precipitation, but not as extensive as the surface soil moisture drying, a pattern also observed in CMIP5 (A. Berg et al., 2017; Cook et al., 2015, 2018). This may be indicative of a longer seasonal memory deeper in the soil column, where antecedent moisture anomalies can more easily carry over from previous seasons, even as near-surface soil moisture is more sensitive to concurrent seasonal changes in evaporative demand and precipitation (A. Berg et al., 2017; Cook et al., 2015). It may also re-

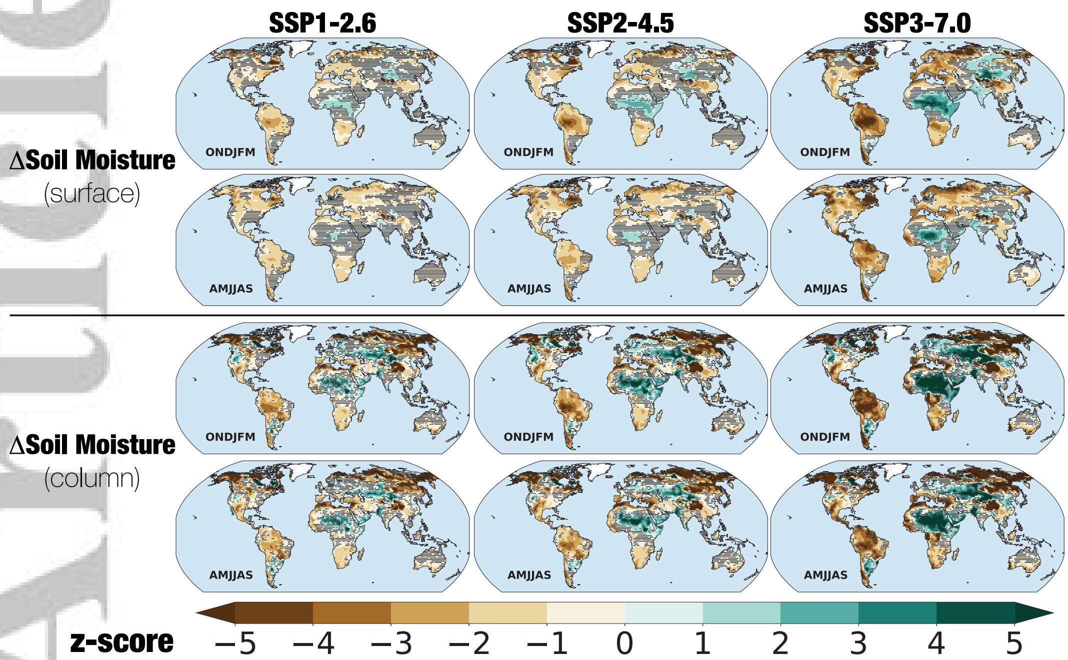

Figure 3. Six-month seasonal average surface (top panels) and total column (bottom panels) soil moisture changes (z-score, 2071-2100 versus 1851–1880) in the SSPs. Areas where changes are non-robust (R<0.90) are indicated by hatching.

flect a reduced sensitivity of deeper soil moisture pools to increases in evaporative demand because of stronger controls by vegetation processes (e.g., increases in water use efficiency with higher atmospheric CO_2 concentrations) (A. Berg et al., 2017). Analyses in some models, however, suggest that divergent trends in shallow versus deep soil moisture responses are not a universal response to warming (Mankin, Smerdon, et al., 2017). Additionally, it should be noted that soil columns across models in our ensemble do not all extend to the same maximum depth, making standardized comparisons of this metric across models more difficult. For example, the bottom of the deepest soil layer in BCC-CSM2-MR extends to 3.57 meters, while in the CNRM family of models the bottom of the deepest layer is 12 meters below the surface (although only hydrologically active down to 8 meters). Regardless, the more extensive drying in both the surface and total column soil moisture diagnostics highlights the importance of processes other than precipitation for understanding future agricultural drought.

3.4 Runoff

In the Northern Hemisphere, runoff declines occur primarily during AMJJAS and are generally associated with increases in runoff over the same regions during ONDJFM, especially at high northern latitudes and in high elevation areas of the mid-latitudes (e.g., montane regions of western North America) (Figure 4). These are regions where, much like in CMIP5, snow dynamics are important, and where the projected seasonal shifts in runoff likely reflect warming impacts on total precipitation (Knutti & Sedlacek, 2013), snow versus rain partitioning (Krasting et al., 2013), and the surface snowpack (Shi & Wang, 2015). Warming increases total precipitation at mid- to high-latitudes in the Northern Hemisphere during the cold season (Figure 2), with an increasing fraction of this precipitation falling as rain rather than snow. At the surface, warming also reduces the water stored in the snowpack (e.g., through lower snowfall inputs and increased losses from

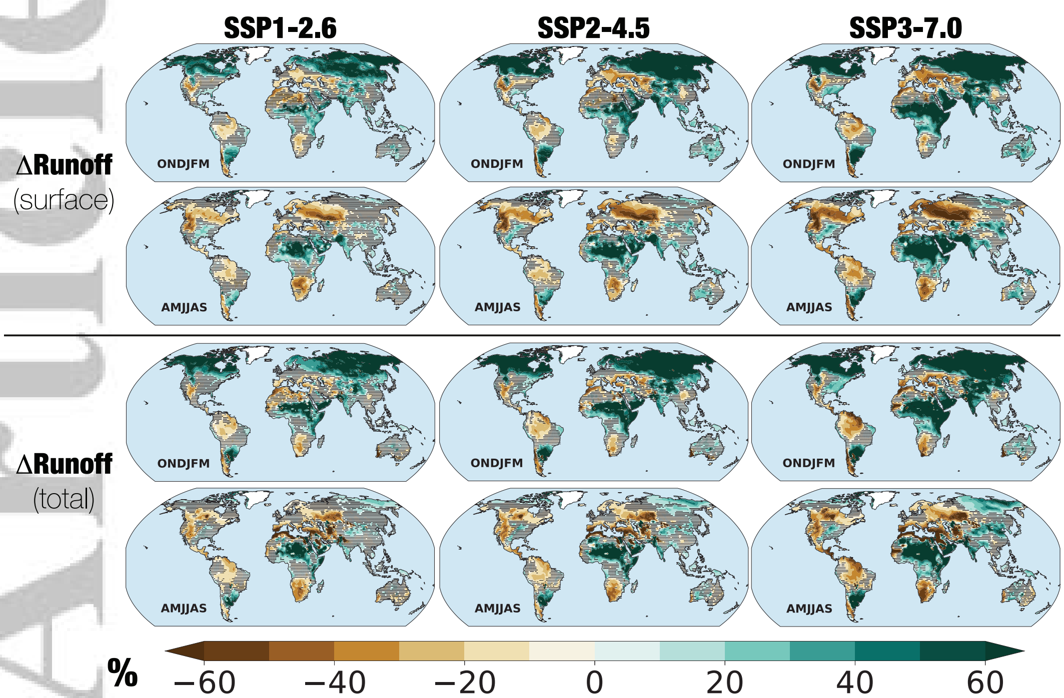

Figure 4. Six-month seasonal average surface (top panels) and total (bottom panels) runoff changes (%, 2071-2100 versus 1851–1880) in the SSPs. Areas where changes are non-robust (R<0.90) are indicated by hatching.

sublimation and melting) and also shifts the timing of snowpack melt earlier in the season. Through these processes, more direct runoff occurs in the winter and early spring, less moisture is stored in the snowpack, and less water is therefore available during the subsequent growing season.

Elsewhere, runoff changes are tied closely to changes in total precipitation. Robust runoff increases occur over most monsoon regions, consistent with the intensification of the monsoons and increases in total monsoon-season precipitation. Runoff also declines in the Mediterranean and other regions with Mediterranean-climates, like southwestern Australia and Chile, as well as over Central America, the Amazon, and southern Africa. As with soil moisture, robust runoff reductions still occur for many regions even under SSP1-2.6 (e.g., western North America, Europe and the Mediterranean, South America, southern Africa), highlighting the strong sensitivity of the terrestrial hydrologic cycle to even modest warming. However, while robust declines in runoff (surface and total) are generally more widespread compared to precipitation, this drying is not as extensive as the soil moisture declines noted previously.

Somewhat paradoxically, certain regions show divergent trends in soil moisture and runoff. For example, over the southeastern United States, Southeast Asia, and southeastern Australia, soil moisture declines under most SSP scenarios while, at the same time, runoff either increases or does not change in a robust manner. This is perhaps not surprising, given the myriad of different processes affecting soil moisture and runoff (Mankin et al., 2019; X. Zhang et al., 2014), but it does further highlight important differences in surface moisture responses across different drought variables.

3.5 Comparisons To CMIP5

To quantify differences between the CMIP6 ensemble and the previous generation of models in CMIP5, we compare the sign of the MME responses in SSP5-8.5 (CMIP6) and RCP 8.5 (CMIP5) (Figure 5). Here, we focus on differences in the sign of the MME ensemble responses, rather than magnitude or robustness, because of the challenges inherent in accounting for potentially important differences in the two ensembles that are unrelated to advances in model physics or process representations (e.g., number of models or ensemble members, specific models included, etc). Disagreements on the sign of the MME response between CMIP5 and CMIP6 are indicated by the colored hatching: red hatching highlights regions where CMIP6 shows drying and CMIP5 is wetting, while blue hatching shows areas where CMIP6 shows wetting and CMIP5 shows drying.

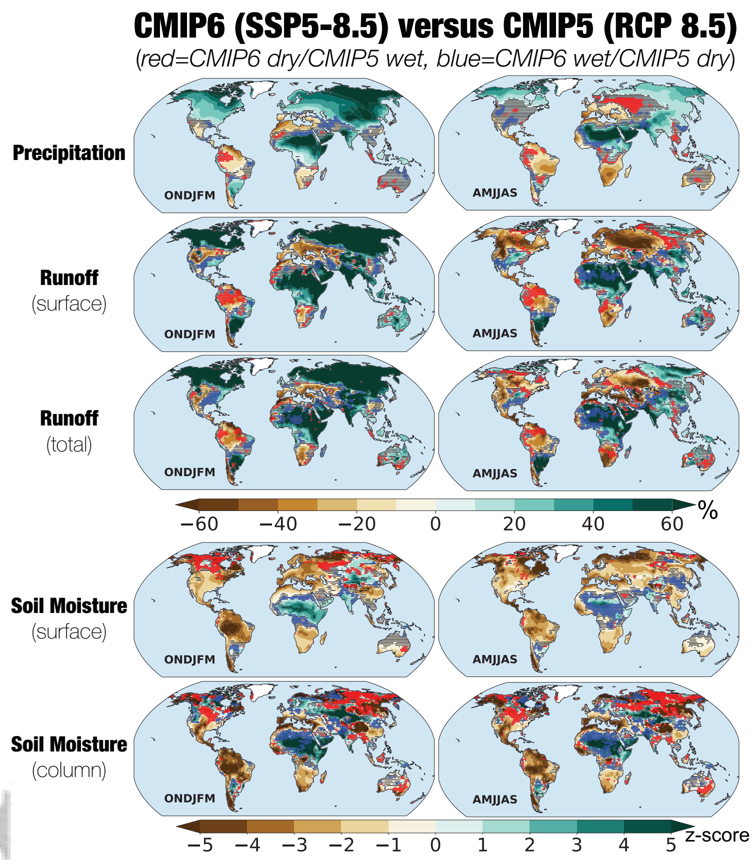

Figure 5. Six-month seasonal average changes (2071–2100 versus 1851–1880) in precipitation (%), surface and total runoff (%), and surface and total column soil moisture (z-score) for SSP5-8.5 in our CMIP6 ensemble. Colored hatching indicates regions where the sign of the MME response (drying or wetting) is different between CMIP6 and a similar ensemble from the RCP 8.5 scenario in CMIP5: red=areas where CMIP6 indicates drying and CMIP5 shows wetting; blue=areas where CMIP6 indicates wetting and CMIP5 shows drying. The 17 Models in the CMIP5 ensemble are: BCC-CSM-1.1, CCSM4, CNRM-CM5, CSIRO-MK3-6.0, CanESM2, GFDL-ESM2G, GFDL-ESM2M, GISS-E2-R, INMCM4, IPSL-CM5A-LR, IPSL-CM5A-MR, IPSL-CM5B-LR, MIROC-ESM, MIROC-ESM-CHEM, MIROC5, MRI-CGCM3, and NorESM1-M.

For most regions, the large-scale patterns of wetting and drying are consistent between CMIP5 and CMIP6, and areas where the two ensembles disagree are primarily in transitional regions between robust drying and wetting responses (e.g., ONDJFM precipitation and surface soil moisture in northern Africa), or in areas where the CMIP6 response is non-robust (e.g., AMJJAS precipitation over the western United States). Over some areas, however, differences between CMIP5 and CMIP6 are spatially extensive, especially in cases where the sign of the change switches to drying in CMIP6: total column soil moisture over Alaska, the Northern Plains of the United States, and northeastern Asia; runoff over the Amazon and southern Africa; and AMJJAS precipitation in eastern Europe. Fewer areas with robust responses see a sign reversal to wetting in CMIP6: runoff in the eastern United States and parts of China; total column soil moisture in northern Africa, the Middle East, and southwestern Asia; and surface soil moisture in northern China, and northern Africa. At present, it is impossible to definitively attribute these differences to any specific reason. More broadly, however, the most robust regional patterns of wetting and drying in CMIP6 are largely consistent with CMIP5.

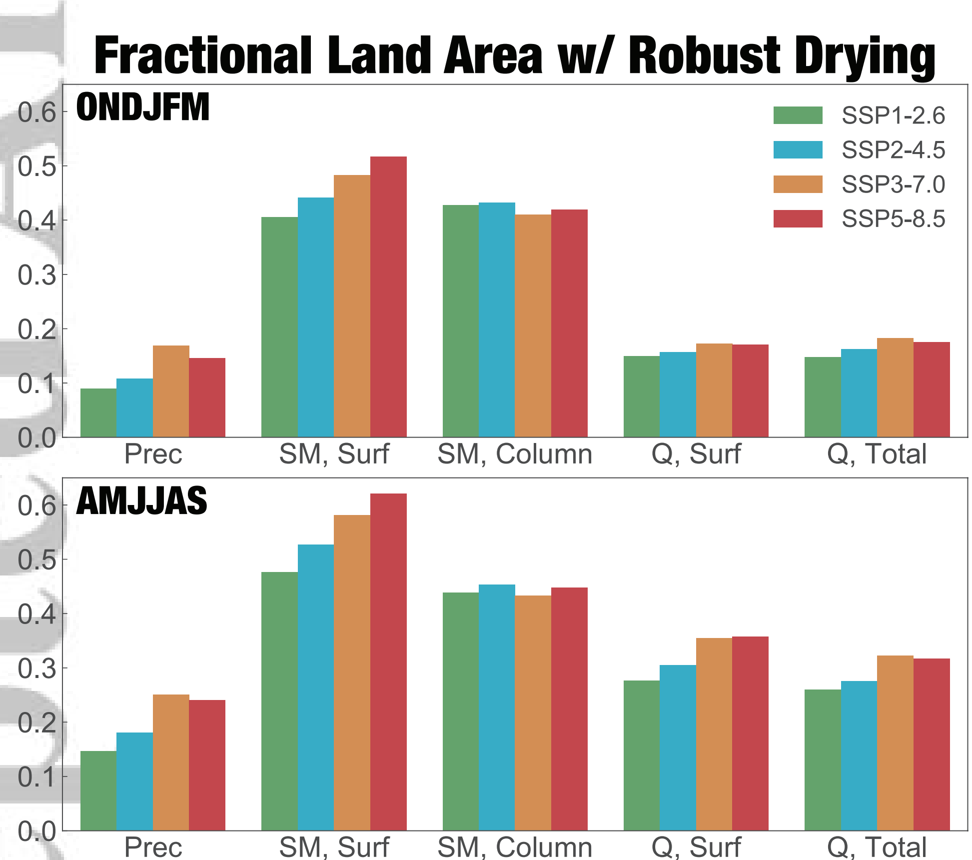

Figure 6. For all drought variables and SSP scenarios, the fractional land area, excluding Antarctica and Greenland, with robust drying responses (defined as areas where $R \geq 0.90$ and the sign of the change is negative) during ONDJFM and AMJJAS.

3.6 Extent of Robust Drying Over Global Land Areas

Excluding Antarctica and Greenland, the global land area that experiences robust drying is sensitive to both the SSP scenarios and drought variables being considered (Figure 6). Within each SSP, the spatial extent of drying is larger for soil moisture and runoff compared to precipitation. During AMJJAS under SSP3-7.0, for example, robust drying in precipitation affects only 25.1% of the land area, increasing to 58.1% for surface soil moisture, 43.4% for total column soil moisture, 35.5% for surface runoff, and 32.3%

for total runoff. To a lesser degree, the spatial extent of drying also increases with the level of forcing in the SSP scenarios, especially in surface soil moisture where drying during AMJJAS increases from 47.7% of the global land area in SSP1-2.6 to 62.1% in SSP5-8.5. Changes in the extent of drying across SSPs is much more muted in precipitation and runoff, however, and effectively zero in the case of total column soil moisture. Increases in the spatial extent of drying with SSP forcing are also relatively small compared to the increasing intensity of drying *within regions* as warming increases (e.g., Figures 2–4). Over the Mediterranean, for example, the intensity of declines in AMJJAS surface runoff is between 10–20% in SSP1-2.6, but exceeds 30–60% for much of the region under SSP3-7.0 and SSP5-8.5.

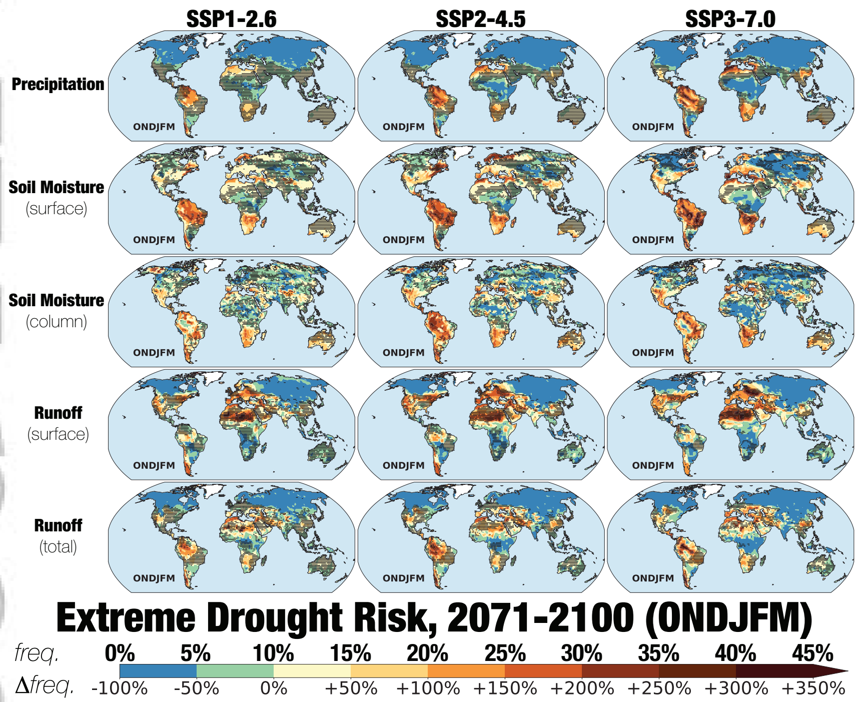

Figure 7. For ONDJFM during 2071–2100, the risk or likelihood of extreme single-year drought events (top numbers, bold text) and the change in risk relative to 1851–1880 (bottom numbers, plain text). Extreme single-year droughts are defined as years, for each variable, with single-year magnitudes equal to or drier than the 10^{th} percentile of all years from the baseline 1851–1880. Hatching indicates areas of non-robust changes in the MME mean, identical to Figures 2–4.

3.7 Changes in Extreme Drought Risk

Shifts in extreme drought risk, defined as years with event magnitudes below the 10^{th} percentile from the 1851–1880 baseline, broadly follow changes in the MME mean (ONDJFM, Figure 7; AMJJAS, Figure 8). The most intense and widespread declines in drought risk occur across high northern latitudes, India, East Africa, and Argentina, all regions that experience some of the largest and most robust increases in MME mean precipitation. Ensemble mean drying in western North America, southern Africa, the Amazon, and Europe causes some of the largest increases in extreme soil moisture and runoff drought risk, as high as +200-300%, equivalent to a x3 to x4 times increase in the likelihood of occurrence of these events. Increases in risk can also be seen in regions that experience either robust wetting in the MME mean (e.g., runoff in East Africa) or where the MME mean response is not robust (e.g., runoff in eastern Australia). While somewhat counterintuitive, this implies that for some regions drought risk may increase even if the mean state does not get drier because the underlying variability increases or becomes increasingly skewed towards the drier tail, a phenomenon also documented in CMIP5 (Pendergrass et al., 2017). As expected, increases in drought risk are largest in the higher warming SSP3-7.0 and SSP5-8.5 scenarios. However, increases in extreme drought risk are large for some variables and regions, even under the lowest warming scenarios. For example, drought risk under SSP1-2.6 increases by over +100% (x2) over western North America, the Amazon, southern Africa, Europe, and the Mediterranean.

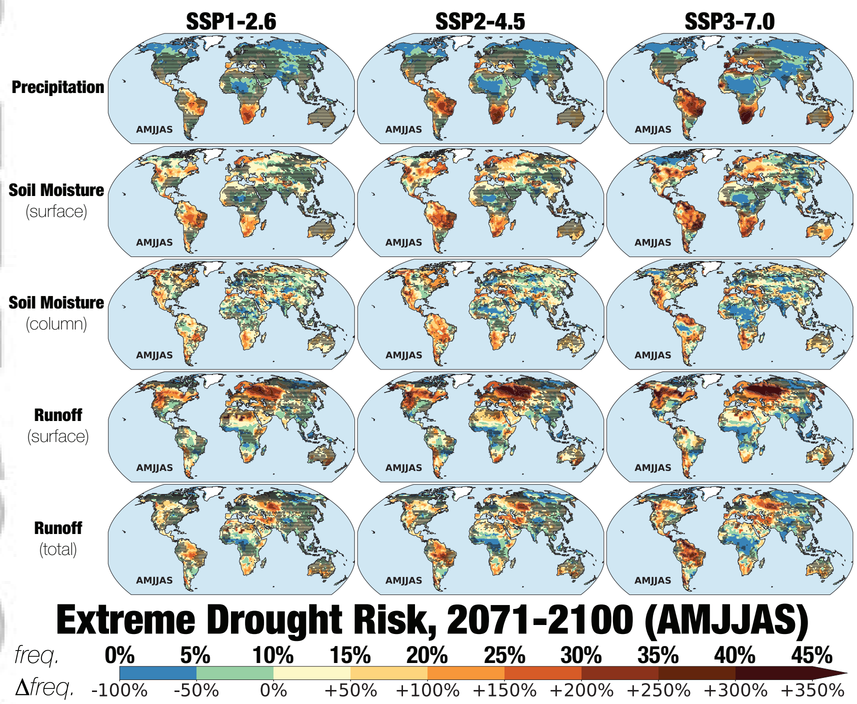

Figure 8. For AMJJAS during 2071–2100, the risk or likelihood of extreme single-year drought events (top numbers, bold text) and the change in risk relative to 1851–1880 (bottom numbers, plain text). Extreme single-year droughts are defined as years, for each variable, with single-year magnitudes equal to or drier than the 10^{th} percentile of all years from the baseline 1851–1880. Hatching indicates areas of non-robust changes in the MME mean, identical to Figures 2–4.

3.8 Annual Average Changes

Despite often divergent trends across seasons, annual average precipitation increases across most regions in the Northern Hemisphere with warming (Figure 9, left column). At mid- to high-latitudes, this is indicative of large increases during the cold season that overcompensate for any declines or marginal responses during the rest of the year (Figure 2). Similarly, intensification of mid- to late-season monsoon rainfall over regions like India and extratropical South America drives increases in total annual precipitation, despite delays in monsoon onset. Robust precipitation declines are still apparent in the same regions from the seasonal plots, including the Amazon, Central America, Mediterranean, southern Africa, and southwest and southeast coastal Australia. Broadly, however, an-

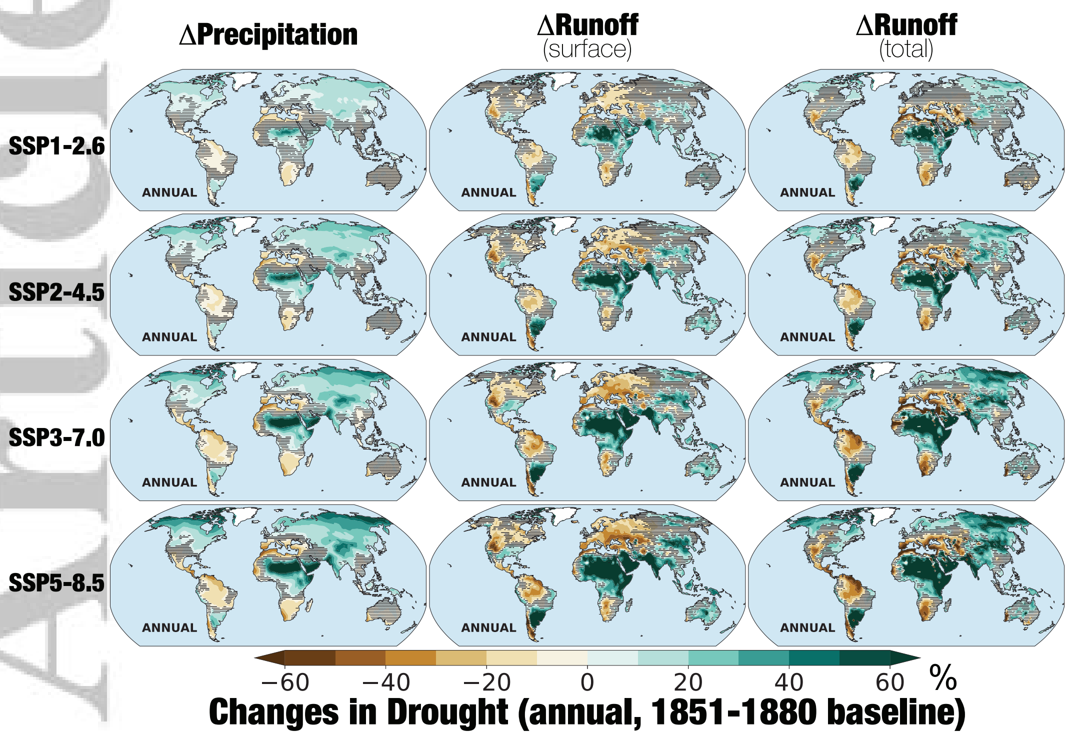

Figure 9. Annual average, multi-model ensemble mean changes (percent) in precipitation and runoff for 2071–2100, using the 1851–1880 baseline. Areas where changes are non-robust (R<0.90) are indicated by hatching.

nual terrestrial precipitation responses are dominated by robust wetting or non-robust responses, with net drying much more localized in specific regions.

Increases in total annual precipitation, however, does not directly translate to increases in total annual runoff for many regions (Figure 9, center and right columns). For example, despite widespread precipitation increases across the mid- to high-northern latitudes, annual surface runoff declines across Europe, western Russia, much of Canada, and the western United States. This is likely attributed primarily to large-scale shifts in precipitation from snow to rain, resulting in a redistribution of runoff from the warm to cold season (see Figure 4) and net declines in the annual average. Over these same regions, annual average declines are not as widespread in total runoff, though they are more intense and extensive over western North America and Europe than would be expected from annual precipitation changes alone. Elsewhere, annual runoff changes generally closely follow the sign of precipitation changes.

Compared to precipitation and runoff, robust declines in soil moisture are much more widespread, affecting large areas of every continent (excluding Antarctica), even in regions with robust increases in total annual precipitation (Figure 10). As noted previously, this likely reflects the myriad of other important processes affecting soil moisture that also change with warming, including increased evaporative demand in the atmosphere and plant water use. The few localized regions experiencing robust increases in annual soil moisture are those areas with some of the strongest increases in precipitation, including extra-tropical South America, northern and eastern Africa, India, and Central Asia.

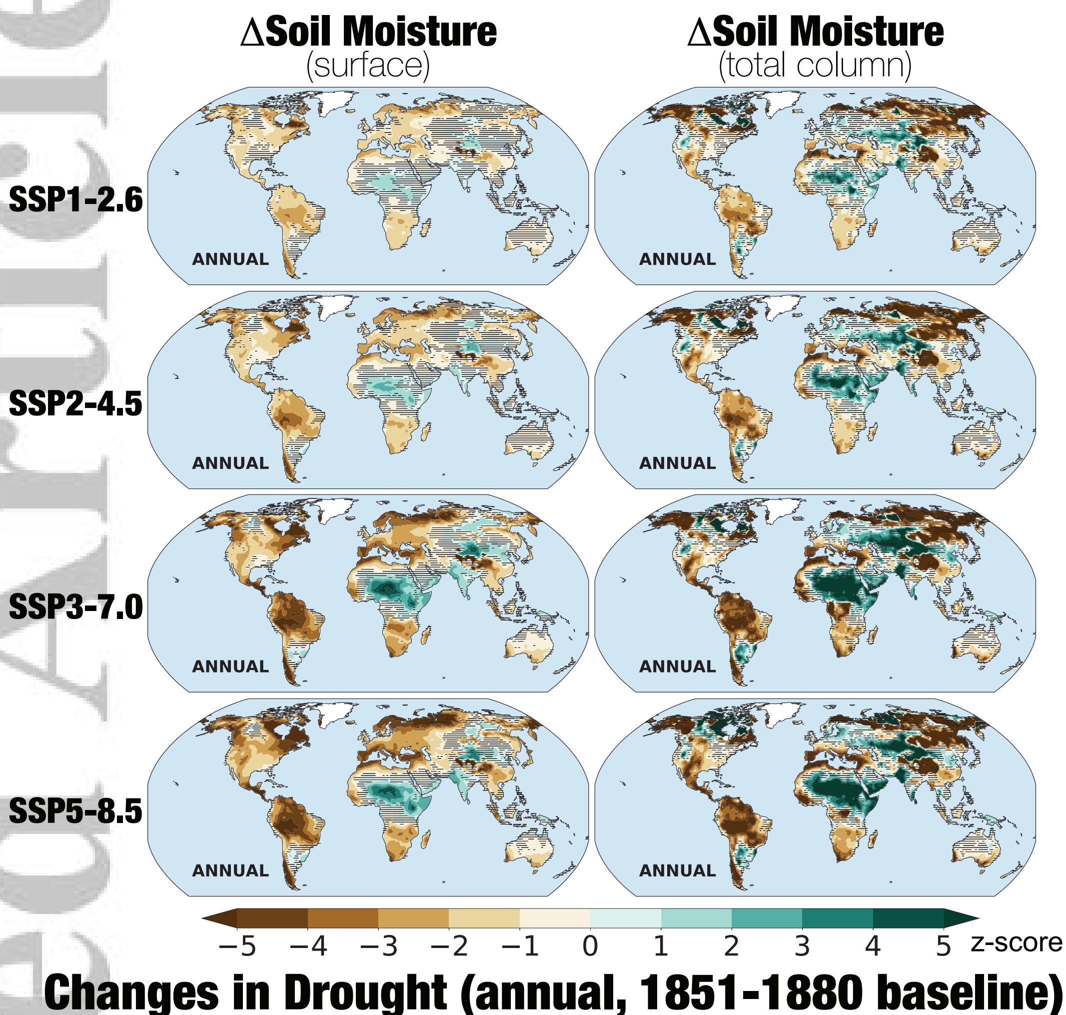

Figure 10. Annual average, multi-model ensemble mean changes (z-score) in surface and total column soil moisture for 2071–2100, using the 1851–1880 baseline. Areas where changes are non-robust (R<0.90) are indicated by hatching.

3.9 Baseline Sensitivity and Future Mitigation Potential

All of our results presented to this point use a near pre-industrial baseline, 1851–1880, for calculation of the anomalies, allowing us to evaluate the full scale of changes in drought associated with anthropogenic climate change. To assess the potential for greenhouse gas mitigation to reduce future drought impacts from climate change, we recalculate the annual average anomalies using a modern baseline from the last 30 years of the historical simulations, 1985–2014. Comparing these anomalies with those using the pre-industrial baseline highlights how the changes in drought associated with warming are distributed between the historical and future intervals, as well as the potential future mitigation benefits for drought from shifting towards lower warming pathways.

In the case of precipitation, it is clear that much of the drying in the SSP1-2.6 and SSP2-4.5 projections is driven by changes during the historical period (Figure 11, left column). For example, many of the regions (e.g., Central America, the Amazon, the Mediter-

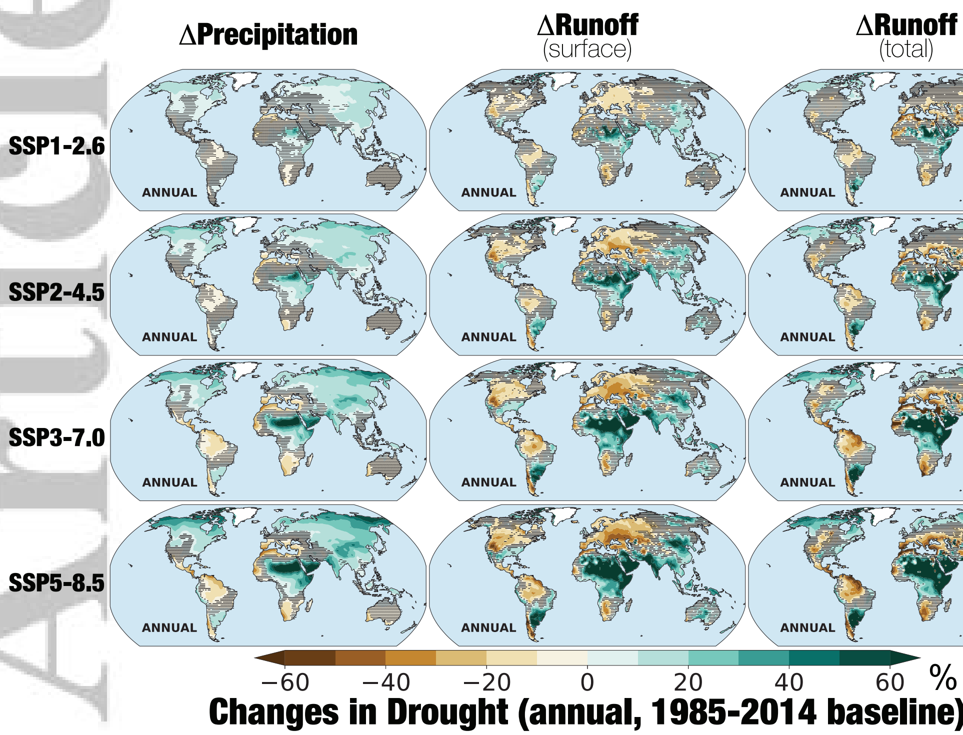

Figure 11. Annual average, multi-model ensemble mean changes (percent) in precipitation and runoff for 2071–2100, using the 1985–2014 baseline. Areas where changes are non-robust (R<0.90) are indicated by hatching.

ranean) with robust annual precipitation declines using the 1851–1880 baseline (Figure 9) are non-robust when using 1985–2014. This suggests that, in terms of meteorological drought, further declines can likely be prevented by following these pathways over the higher warming scenarios of SSP3-7.0 and SSP5-8.5, where continued precipitation reductions in many regions are likely.

Following these lower forcing pathways would also substantially diminish future declines in runoff (Figure 11, center and right columns) and soil moisture (Figure 12) compared to SSP3-7.0 and SSP5-8.5. However, unlike with precipitation where additional future drying is mostly prevented in these low warming scenarios, there are still substantial and robust future declines in runoff and soil moisture, even in regions where precipitation responses are non-robust (e.g., the western United States). This again highlights the importance of non-precipitation processes for agricultural and hydrological drought. Furthermore, this suggests that, even under the most optimistic forcing pathways, mitigation will be insufficient to completely address drought responses to climate change, and some degree of adaptation will be necessary to increase resiliency in a drier future.

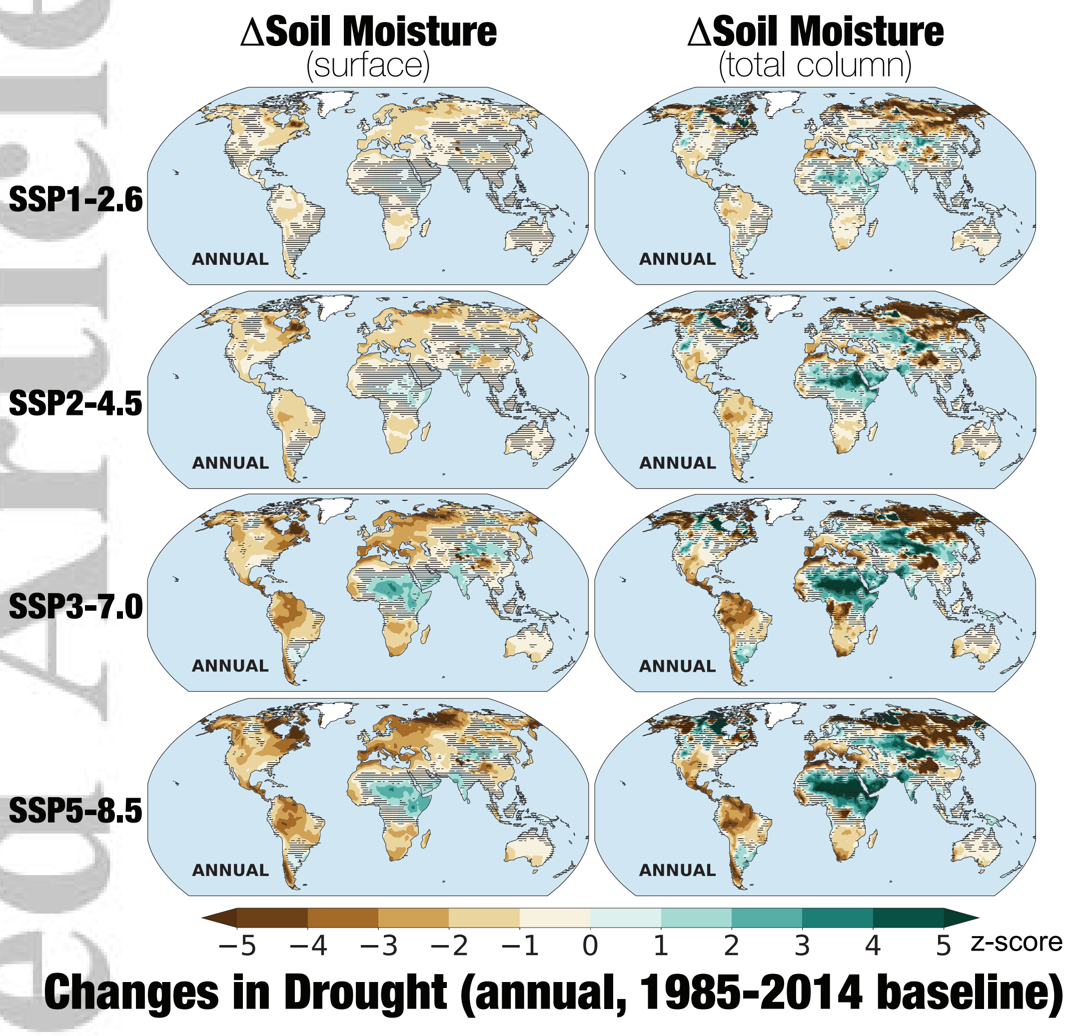

Figure 12. Annual average, multi-model ensemble mean changes (z-score) in surface and total column soil moisture for 2071–2100, using the 1985–2014 baseline. Areas where changes are non-robust ($R<0.90$) are indicated by hatching.

4 Conclusions

Understanding how drought dynamics will change in a warming world is an area of active research involving a complex range of processes (e.g., precipitation, evapotranspiration, plant physiological responses) that transcend traditional disciplinary boundaries (e.g., hydrology, ecology, climatology) (A. Berg et al., 2017; Cook et al., 2018; Dai et al., 2018; Mankin et al., 2019; Milly & Dunne, 2016; Swann, 2018). Much of our current knowledge and expectations for how drought will change over the coming decades originates in analyses of large climate model ensembles, including those simulations organized as part of CMIP5 during the most recent Fifth Assessment Report from the Intergovernmental Panel on Climate Change (IPCC) (IPCC, 2013). In anticipation of the upcoming Sixth Assessment Report from the IPCC, we investigated drought responses to warming across different drought variables, seasons, and future forcing scenarios at the global-scale in the latest, state-of-the-art climate model projections in CMIP6. We found that:

- The sign and magnitude of drought responses to warming depends heavily on the region, season, and indicators being considered.
- Robust drying responses in soil moisture and runoff are more widespread compared to precipitation, especially during AMJJAS in the Northern Hemisphere. For runoff, this is mostly likely a consequence of warming effects on snow that cause a redistribution of runoff from the warm to cool season. In the case of soil moisture, it is likely connected to increases in evaporative demand mediated by surface vegetation responses and water use.
- The spatial extent of robust drying increases under the higher forcing and warming scenarios in most variables, with surface soil moisture showing the strongest response. Compared to the spatial extent of the drying, however, the response *within* robustly drying regions is much more sensitive, with drying increasing sharply under higher warming scenarios.
- At the same time, some regions are likely to see reductions in drought, especially areas where total annual precipitation increases, including the high northern latitudes and monsoon regions on all continents. This robust wetting is more intense and widespread in the precipitation and runoff response compared to soil moisture.
- Beyond changes in the mean state (Figures 2–4), the CMIP6 models also show changes in the risk or likelihood of the historically most extreme drought events (Figures 7–8). The risk of these events generally increases in areas of robust mean drying and decreases in regions of robust mean wetting, suggesting that increases in these extreme events are largely driven by shifts in the mean. However, certain regions (e.g., East Africa, eastern Australia) show increased extreme drought risk despite either non-robust mean moisture responses or even shifts toward wetter average conditions, indicating changes in variability or the shape of the underlying distributions.
- Results from CMIP6 are broadly consistent with CMIP5, at least in the sign of the response. This suggests that many of the same physical processes and underlying uncertainties will remain important for interpreting the latest model projections. Understanding areas where there is divergence between CMIP5 and CMIP6, however, will require more detailed investigations to determine the most likely reasons (e.g., structural changes in the models, differences in the underlying climate sensitivity, internal variability, etc.).
- Even with differences across drought variables and seasons, major hotspots of consistent drying with warming are apparent in CMIP6, including western North America, Europe and the Mediterranean, Central America, South America (outside of Argentina), southern Africa, and southwestern and southeastern Australia. Encouragingly, because the severity of future drying in most regions is strongly connected to the forcing scenario, there are substantial mitigation benefits to following a lower emissions pathway. Even under SSP1-2.6 and SSP2-4.5, however, robust increases in drought relative to the present-day can still be expected for many regions.

Despite major developments in land surface models between CMIP5 and CMIP6 (e.g., Li et al., 2019), regional drought responses are remarkably consistent between the two ensembles (Figure 5). At the same time, it remains important to determine whether the increased sophistication in CMIP6 models represents a meaningful improvement over CMIP5, and whether these improvements and the consistency between CMIP5 and CMIP6 offers a case for increased confidence in these results. Preliminary results from the International Land Model Benchmarking Project (ILAMB, `https://www.ilamb.org/results/`) show that the CMIP6 ensemble improves performance, relative to observations, over CMIP5 in a number of drought-related processes, from ecosystem processes like prognostic leaf area index, to hydrologic processes like runoff, terrestrial water storage, and surface energy partitioning. Relative to observations, however, there is not yet a clear CMIP6 improvement in temperature and precipitation. With these improvements in CMIP6, is it reasonable to expect drought risks to be better-constrained, or their uncertainties reduced? Given the critical role of internal variability and other irreducible uncertainties in drought risk assessments (Coats & Mankin, 2016), it is unlikely. Model improvements and better representations of drought processes, while important, therefore should not be expected to directly translate to reduced uncertainties in drought risk projections.

Due to the consistency between the two model generations, our CMIP6 analysis largely reaffirms conclusions from studies using CMIP5 (as reviewed in Cook et al. (2018)), highlighting many of the same regions likely to be most at risk for increased drought in a warmer future and areas where hydroclimate responses are either non-robust or shift towards wetter conditions. Our results underline the importance of considering both the seasonality of drought responses, and the differences in sign, magnitude, and robustness of changes across different drought variables. Such details are especially important when trying to connect drought in the hydrologic cycle to the actual effect of these moisture deficits on people and ecosystems. Runoff, for example, encompasses the main sphere of active human water resources management, the primary source for reservoirs, hydropower, and irrigation. Conversely, soil moisture is the most critical variable for supplying ecosystems and rainfed agriculture. As is apparent in the SSP projections, however, soil moisture and runoff show substantially different responses to climate change. These variables therefore cannot substitute as proxies for each other, underscoring the necessity of considering the full hydrologic cycle response to warming.

Confidence in drought projections requires validating drought dynamics, variability, and trends within climate models, an often difficult task. One major limitation is the lack of long-term, high quality instrumental drought observations. Precipitation data is often only sparsely available for many regions outside of Europe and the United States, especially prior to 1950, and other variables (e.g., soil moisture, runoff) are typically unavailable at scales comparable to the typical resolution of climate model grid cells. Additionally, many of the important processes affecting drought variability and trends in climate models are only weakly constrained. This includes evapotranspiration (Lian et al., 2018; Y. Zhang et al., 2016), vegetation responses to drought and climate (Green et al., 2019; Mankin et al., 2019), the fidelity of simulated precipitation and associated teleconnections (Allen & Anderson, 2018; Coats et al., 2013; Tierney et al., 2015; B. Zhang & Soden, 2019), and regional feedbacks and interactions that may amplify or ameliorate drought responses (A. Berg et al., 2016; Zhou et al., 2019). In part because of these important uncertainties, numerous studies have highlighted the limitations of climate models in their ability to adequately simulate drought and raised concerns regarding their utility for climate change applications (Huang et al., 2016; Lehner et al., 2019; Nasrollahi et al., 2015; Orlowsky & Seneviratne, 2013; Padrón et al., 2019; Ukkola, De Kauwe, et al., 2016; Ukkola et al., 2018).

Despite these weaknesses, there is evidence that observed drought trends and events, and the associated climate change mechanisms, are consistent with the trends and mechanisms simulated within climate models. In terms of precipitation, the most robust drying in the CMIP6 projections occurs in Mediterranean-type climate regions around the world, the same regions where long-term precipitation declines and increases in meteorological drought have been observed (Seager et al., 2019). This includes the Mediterranean and southern Europe (Gudmundsson & Seneviratne, 2016; Hoerling et al., 2012; Kelley et al., 2015), southern Africa (Otto et al., 2018), Chile (Garreaud et al., 2020), and southwest Australia (Delworth & Zeng, 2014). Despite strong drying over Central America and the Caribbean in CMIP6, however, recent precipitation trends in this region cannot be currently separated from natural variability (Anderson et al., 2019; Jones et al., 2016), even as warming may be amplifying soil moisture drought over the Caribbean (Herrera et al., 2018). Similarly, there is strong evidence for the western United States that warming temperatures and increased atmospheric evaporative demand have contributed to soil moisture and runoff drying (Griffin & Anchukaitis, 2014; Hoell et al., 2019; McCabe et al., 2017; Williams et al., 2015; Xiao et al., 2018) and declining snowpacks

(Barnett et al., 2008; N. Berg & Hall, 2017; Mote et al., 2016, 2018), even as the recent precipitation declines have been attributed primarily to natural variability (Delworth et al., 2015; Lehner et al., 2018; Seager et al., 2015). Model responses indicating that warming will increase vegetation water use and help drive surface drying (Mankin et al., 2019) are also broadly supported by observations (Trancoso et al., 2017; Ukkola, Prentice, et al., 2016). Further, concurrent wetting and drying trends in soil moisture across regions are also consistent between climate models and observations at the near-global scale, and in line with the expected responses to warming over the 20th century (Gu et al., 2019; Marvel et al., 2019). Thus, despite the documented weaknesses and uncertainties in the climate models, the broad consistency between models and observations over many regions provides some increased confidence in their value for investigating drought and climate change.

Finally, the clear increase in the magnitude and extent of drying as the forcing and warming increases across the SSPs demonstrates the clear benefits of greenhouse gas mitigation for reducing climate change forced increases in drought risk and severity, a result also demonstrated in CMIP5 (Ault et al., 2016). However, we find that robust and large-magnitude drying is not isolated to the higher-end scenarios of SSP3-7.0 and SSP5-8.5, but exists even under the more aggressive SSP1-2.6 and SSP2-4.5 mitigation pathways, similar to results found by Lehner et al. (2017) using CMIP5. This includes regions like western North America, the Mediterranean, southern Africa, and the Amazon (Figures 11 and 12). Furthermore, even though the SSP1-2.6 drying in the MME mean may appear modest, these relatively small changes in the mean state still translate to large shifts in tail risks. For example, over much of western North America under SSP1-2.6, the frequency of extreme soil moisture and surface runoff droughts during the warm season (AMJJAS) increases by 100–200% (a factor of x2 to x3) (Figures 7 and 8). Thus, even in the scenario that limits end of the 21st century warming to +2 K above pre-industrial, these mitigation efforts will still result in substantial increases in drought risk and severity, indicating that adaptation measures will still be required to ensure adequate resiliency in the future.

Acknowledgments

All data from CMIP6 simulations used in our analyses are freely available from the Earth System Grid Federation (`https://esgf-node.llnl.gov/search/cmip6/`). BI Cook, K Marvel, and AP Williams were all supported by the NOAA MAPP grant, "Integrating models, paleoclimate, and recent observations to develop process-level understanding of projected changes in US drought". This work benefited from participation by BI Cook, K Marvel, and AP Williams in the NOAA CMIP6 Task Force. The authors thank Naomi Henderson and Haibo Liu at the Lamont-Doherty Earth Observatory for essential help organizing output from the CMIP6 models. HadCRUT data are freely available from `https://crudata.uea.ac.uk/cru/data/temperature/`. The authors thank two anonymous reviewers for helpful comments that improved this manuscript. Lamont contribution #XXXX.

References

Allen, R. J., & Anderson, R. G. (2018). 21st century California drought risk linked to model fidelity of the El Niño teleconnection. *npj Climate and Atmospheric Science*, *1*(1), 21. doi: 10.1038/s41612-018-0032-x

Anderson, T. G., Anchukaitis, K. J., Pons, D., & Taylor, M. (2019). Multiscale trends and precipitation extremes in the Central American Midsummer Drought. , *14*(12), 124016. Retrieved from `http://dx.doi.org/10.1088/1748-9326/ab5023` doi: 10.1088/1748-9326/ab5023

Ault, T. R., Mankin, J. S., Cook, B. I., & Smerdon, J. E. (2016). Relative impacts of mitigation, temperature, and precipitation on 21st-century megadrought risk in the American Southwest. *Science Advances*, *2*(10). doi:

10.1126/sciadv.1600873

Barnett, T. P., Pierce, D. W., Hidalgo, H. G., Bonfils, C., Santer, B. D., Das, T., ... others (2008). Human-induced changes in the hydrology of the western United States. *Science*, *319*(5866), 1080–1083. doi: 10.1126/science.1152538

Berg, A., Findell, K., Lintner, B., Giannini, A., Seneviratne, S. I., van den Hurk, B., ... Milly, P. C. D. (2016, 05 16). Land-atmosphere feedbacks amplify aridity increase over land under global warming. *Nature Climate Change*, *advance online publication*, –.

Berg, A., Sheffield, J., & Milly, P. C. D. (2017). Divergent surface and total soil moisture projections under global warming. *Geophysical Research Letters*, *44*(1), 236–244. Retrieved from http://dx.doi.org/10.1002/2016GL071921 doi: 10.1002/2016GL071921

Berg, N., & Hall, A. (2017). Anthropogenic warming impacts on California snowpack during drought. *Geophysical Research Letters*, *44*(5), 2511–2518. doi: 10.1002/2016GL072104

Boucher, O., Denvil, S., Caubel, A., & Foujols, M. A. (2018). IPSL IPSL-CM6A-LR model output prepared for CMIP6 CMIP. Retrieved from https://doi.org/10.22033/ESGF/CMIP6.1534 doi: 10.22033/ESGF/CMIP6.1534

Breshears, D. D., Carroll, C. J. W., Redmond, M. D., Wion, A. P., Allen, C. D., Cobb, N. S., ... Newell-Bauer, O. (2018). A Dirty Dozen Ways to Die: Metrics and Modifiers of Mortality Driven by Drought and Warming for a Tree Species. *Frontiers in Forests and Global Change*, *1*, 4. Retrieved from https://www.frontiersin.org/article/10.3389/ffgc.2018.00004 doi: 10.3389/ffgc.2018.00004

Byrne, M. P., & O'Gorman, P. A. (2015, 2019/11/11). The Response of Precipitation Minus Evapotranspiration to Climate Warming: Why the "Wet-Get-Wetter, Dry-Get-Drier"Scaling Does Not Hold over Land. *Journal of Climate*, *28*(20), 8078–8092. doi: 10.1175/JCLI-D-15-0369.1

Coats, S., & Mankin, J. S. (2016, 2020/03/05). The challenge of accurately quantifying future megadrought risk in the American Southwest. *Geophysical Research Letters*, *43*(17), 9225–9233. Retrieved from https://doi.org/10.1002/2016GL070445 doi: 10.1002/2016GL070445

Coats, S., Smerdon, J. E., Cook, B. I., & Seager, R. (2013). Stationarity of the tropical pacific teleconnection to North America in CMIP5/PMIP3 model simulations. *Geophysical Research Letters*, *40*(18), 4927–4932. doi: 10.1002/grl.50938

Cook, B. I., Ault, T. R., & Smerdon, J. E. (2015). Unprecedented 21st century drought risk in the American Southwest and Central Plains. *Science Advances*, *1*(1). doi: 10.1126/sciadv.1400082

Cook, B. I., Mankin, J. S., & Anchukaitis, K. J. (2018, Jun 01). Climate Change and Drought: From Past to Future. *Current Climate Change Reports*, *4*(2), 164–179. Retrieved from https://doi.org/10.1007/s40641-018-0093-2 doi: 10.1007/s40641-018-0093-2

Cook, B. I., Smerdon, J. E., Seager, R., & Coats, S. (2014). Global Warming and 21st century drying. *Climate Dynamics*, *43*(9-10), 2607-2627. doi: 10.1007/s00382-014-2075-y

Dai, A. (2013, 01). Increasing drought under global warming in observations and models. *Nature Climate Change*, *3*(1), 52–58. doi: 10.1038/nclimate1633

Dai, A., Zhao, T., & Chen, J. (2018). Climate change and drought: a precipitation and evaporation perspective. *Current Climate Change Reports*, *4*(3), 301–312. Retrieved from https://doi.org/10.1007/s40641-018-0101-6 doi: 10.1007/s40641-018-0101-6

Danabasoglu, G. (2019a). NCAR CESM2 model output prepared for CMIP6 CMIP historical. Retrieved from https://doi.org/10.22033/ESGF/CMIP6.7627 doi: 10.22033/ESGF/CMIP6.7627

Danabasoglu, G. (2019b). NCAR CESM2-WACCM model output prepared for CMIP6 CMIP amip. Retrieved from `https://doi.org/10.22033/ESGF/CMIP6.10041` doi: 10.22033/ESGF/CMIP6.10041

Delworth, T. L., & Zeng, F. (2014, 08). Regional rainfall decline in Australia attributed to anthropogenic greenhouse gases and ozone levels. *Nature Geoscience*, *7*(8), 583–587. doi: 10.1038/ngeo2201

Delworth, T. L., Zeng, F., Rosati, A., Vecchi, G. A., & Wittenberg, A. T. (2015, 2015/07/23). A Link between the Hiatus in Global Warming and North American Drought. *Journal of Climate*, *28*(9), 3834–3845. doi: 10.1175/JCLI-D-14-00616.1

Eyring, V., Bony, S., Meehl, G. A., Senior, C., Stevens, B., Stouffer, R. J., & Taylor, K. E. (2016). Overview of the coupled model intercomparison project phase 6 (cmip6) experimental design and organisation. *Geoscientific Model Development Discussions*, *8*, 1937-1958. doi: 10.5194/gmdd-8-10539-2015

Garreaud, R., Boisier, J. P., Rondanelli, R., Montecinos, A., Sepúlveda, H. H., & Veloso-Aguila, D. (2020, 2020/03/03). The Central Chile Mega Drought (2010–2018): A climate dynamics perspective. *International Journal of Climatology*, *40*(1), 421–439. Retrieved from `https://doi.org/10.1002/joc.6219` doi: 10.1002/joc.6219

Good, P., Sellar, A., Tang, Y., Rumbold, S., Ellis, R., Kelley, D., & Kuhlbrodt, T. (2019). MOHC UKESM1.0-LL model output prepared for CMIP6 ScenarioMIP ssp245. Retrieved from `https://doi.org/10.22033/ESGF/CMIP6.6339` doi: 10.22033/ESGF/CMIP6.6339

Gosling, S. N., & Arnell, N. W. (2016). A global assessment of the impact of climate change on water scarcity. *Climatic Change*, *134*(3), 371–385. Retrieved from `https://doi.org/10.1007/s10584-013-0853-x` doi: 10.1007/s10584-013-0853-x

Green, J. K., Seneviratne, S. I., Berg, A. M., Findell, K. L., Hagemann, S., Lawrence, D. M., & Gentine, P. (2019). Large influence of soil moisture on long-term terrestrial carbon uptake. *Nature*, *565*(7740), 476–479. Retrieved from `https://doi.org/10.1038/s41586-018-0848-x` doi: 10.1038/s41586-018-0848-x

Greve, P., Orlowsky, B., Mueller, B., Sheffield, J., Reichstein, M., & Seneviratne, S. I. (2014, 09 14). Global assessment of trends in wetting and drying over land. *Nature Geoscience*, *7*, 716 EP -. Retrieved from `https://doi.org/10.1038/ngeo2247` doi: 10.1038/ngeo2247

Griffin, D., & Anchukaitis, K. J. (2014). How unusual is the 2012–2014 California drought? *Geophysical Research Letters*, 2014GL062433. doi: 10.1002/2014GL062433

Gu, X., Zhang, Q., Li, J., Singh, V. P., Liu, J., Sun, P., & Cheng, C. (2019, 2019/12/16). Attribution of Global Soil Moisture Drying to Human Activities: A Quantitative Viewpoint. *Geophysical Research Letters*, *46*(5), 2573–2582. doi: 10.1029/2018GL080768

Gudmundsson, L., & Seneviratne, S. I. (2016). Anthropogenic climate change affects meteorological drought risk in europe. *Environmental Research Letters*, *11*(4), 044005. doi: 10.1088/1748-9326/11/4/044005

Guo, H., John, J. G., Blanton, C., McHugh, C., Nikonov, S., Radhakrishnan, A., ... Zhao, M. (2018). NOAA-GFDL GFDL-CM4 model output. Retrieved from `https://doi.org/10.22033/ESGF/CMIP6.1402` doi: 10.22033/ESGF/CMIP6.1402

Held, I. M., & Soden, B. J. (2006). Robust Responses of the Hydrological Cycle to Global Warming. *Journal of Climate*, *19*(21), 5686–5699. doi: http://dx.doi.org/10.1175/JCLI3990.1

Herrera, D. A., Ault, T. R., Fasullo, J. T., Coats, S. J., Carrillo, C. M., Cook, B. I., & Williams, A. P. (2018, 2020/03/05). Exacerbation of the 2013–2016 Pan-

Caribbean Drought by Anthropogenic Warming. *Geophysical Research Letters*, *45*(19), 10,619–10,626. Retrieved from https://doi.org/10.1029/2018GL079408 doi: 10.1029/2018GL079408

Hessl, A. E., Anchukaitis, K. J., Jelsema, C., Cook, B., Byambasuren, O., Leland, C., … Hayles, L. A. (2018). Past and future drought in Mongolia. *Science Advances*, *4*(3), e1701832. doi: 10.1126/sciadv.1701832

Hoell, A., Perlwitz, J., Dewes, C., Wolter, K., Rangwala, I., Quan, X.-W., & Eischeid, J. (2019). Anthropogenic contributions to the intensity of the 2017 United States northern Great Plains drought. *Bulletin of the American Meteorological Society*, *100*(1), S19–S24. doi: DOI:10.1175/BAMS-D-18-0127.1

Hoerling, M., Eischeid, J., Perlwitz, J., Quan, X., Zhang, T., & Pegion, P. (2012, 2014/10/14). On the Increased Frequency of Mediterranean Drought. *Journal of Climate*, *25*(6), 2146–2161. doi: 10.1175/JCLI-D-11-00296.1

Huang, Y., Gerber, S., Huang, T., & Lichstein, J. W. (2016, 2020/03/03). Evaluating the drought response of CMIP5 models using global gross primary productivity, leaf area, precipitation, and soil moisture data. *Global Biogeochemical Cycles*, *30*(12), 1827–1846. Retrieved from https://doi.org/10.1002/2016GB005480 doi: 10.1002/2016GB005480

Humphrey, V., Zscheischler, J., Ciais, P., Gudmundsson, L., Sitch, S., & Seneviratne, S. I. (2018). Sensitivity of atmospheric CO2 growth rate to observed changes in terrestrial water storage. *Nature*, *560*(7720), 628–631. doi: 10.1038/s41586-018-0424-4

IPCC. (2013). *Climate change 2013: The physical science basis. contribution of working group i to the fifth assessment report of the intergovernmental panel on climate change.* Cambridge, United Kingdom and New York, NY, USA: Cambridge University Press. doi: 10.1017/CBO9781107415324

Jones, P. D., Harpham, C., Harris, I., Goodess, C. M., Burton, A., Centella-Artola, A., … Baur, T. (2016, 2020/03/05). Long-term trends in precipitation and temperature across the Caribbean. *International Journal of Climatology*, *36*(9), 3314–3333. Retrieved from https://doi.org/10.1002/joc.4557 doi: 10.1002/joc.4557

Kelley, C. P., Mohtadi, S., Cane, M. A., Seager, R., & Kushnir, Y. (2015). Climate change in the Fertile Crescent and implications of the recent Syrian drought. *Proceedings of the National Academy of Sciences*, *112*(11), 3241-3246. doi: 10.1073/pnas.1421533112

Knutti, R., & Sedlacek, J. (2013, 04). Robustness and uncertainties in the new CMIP5 climate model projections. *Nature Climate Change*, *3*(4), 369–373. doi: 10.1038/nclimate1716

Krasting, J. P., Broccoli, A. J., Dixon, K. W., & Lanzante, J. R. (2013, 2019/11/12). Future Changes in Northern Hemisphere Snowfall. *Journal of Climate*, *26*(20), 7813–7828. Retrieved from https://doi.org/10.1175/JCLI-D-12-00832.1 doi: 10.1175/JCLI-D-12-00832.1

Krasting, J. P., John, J. G., Blanton, C., McHugh, C., Nikonov, S., Radhakrishnan, A., … Zhao, M. (2018). NOAA-GFDL GFDL-ESM4 model output prepared for CMIP6 CMIP historical. Retrieved from https://doi.org/10.22033/ESGF/CMIP6.8597 doi: 10.22033/ESGF/CMIP6.8597

Lee, J.-Y., & Wang, B. (2014). Future change of global monsoon in the CMIP5. *Climate Dynamics*, *42*(1), 101–119. doi: 10.1007/s00382-012-1564-0

Lehner, F., Coats, S., Stocker, T. F., Pendergrass, A. G., Sanderson, B. M., Raible, C. C., & Smerdon, J. E. (2017). Projected drought risk in 1.5 °C and 2 °C warmer climates. *Geophysical Research Letters*, *44*(14), 7419–7428. doi: doi:10.1002/2017GL074117

Lehner, F., Deser, C., Simpson, I. R., & Terray, L. (2018). Attributing the U.S. Southwest's Recent Shift Into Drier Conditions. *Geophysical Research Letters*, *45*(12), 6251–6261. doi: doi:10.1029/2018GL078312

Lehner, F., Wood, A. W., Vano, J. A., Lawrence, D. M., Clark, M. P., & Mankin, J. S. (2019). The potential to reduce uncertainty in regional runoff projections from climate models. *Nature Climate Change*, *9*(12), 926–933. Retrieved from `https://doi.org/10.1038/s41558-019-0639-x` doi: 10.1038/s41558-019-0639-x

Lemordant, L., Gentine, P., Swann, A. S., Cook, B. I., & Scheff, J. (2018, 04). Critical impact of vegetation physiology on the continental hydrologic cycle in response to increasing co₂. *Proceedings of the National Academy of Sciences*, *115*(16), 4093. doi: 10.1073/pnas.1720712115

Li, W., Zhang, Y., Shi, X., Zhou, W., Huang, A., Mu, M., … Ji, J. (2019). Development of Land Surface Model BCC_AVIM2.0 and Its Preliminary Performance in LS3MIP/CMIP6. *Journal of Meteorological Research*, *33*(5), 851–869. Retrieved from `https://doi.org/10.1007/s13351-019-9016-y` doi: 10.1007/s13351-019-9016-y

Lian, X., Piao, S., Huntingford, C., Li, Y., Zeng, Z., Wang, X., … Wang, T. (2018). Partitioning global land evapotranspiration using CMIP5 models constrained by observations. *Nature Climate Change*, *8*(7), 640–646. Retrieved from `https://doi.org/10.1038/s41558-018-0207-9` doi: 10.1038/s41558-018-0207-9

Mankin, J. S., Seager, R., Smerdon, J. E., Cook, B. I., & Williams, A. P. (2019). Mid-latitude freshwater availability reduced by projected vegetation responses to climate change. *Nature Geoscience*. doi: 10.1038/s41561-019-0480-x

Mankin, J. S., Smerdon, J. E., Cook, B. I., Williams, A. P., & Seager, R. (2017, 2017/10/30). The Curious Case of Projected Twenty-First-Century Drying but Greening in the American West. *Journal of Climate*, *30*(21), 8689–8710. doi: 10.1175/JCLI-D-17-0213.1

Mankin, J. S., Viviroli, D., Mekonnen, M. M., Hoekstra, A. Y., Horton, R. M., Smerdon, J. E., & Diffenbaugh, N. S. (2017). Influence of internal variability on population exposure to hydroclimatic changes. *Environmental Research Letters*, *12*(4), 044007. doi: https://doi.org/10.1088/1748-9326/aa5efc

Marvel, K., Cook, B. I., Bonfils, C. J. W., Durack, P. J., Smerdon, J. E., & Williams, A. P. (2019). Twentieth-century hydroclimate changes consistent with human influence. *Nature*, *569*(7754), 59–65. doi: 10.1038/s41586-019-1149-8

McCabe, G. J., Wolock, D. M., Pederson, G. T., Woodhouse, C. A., & McAfee, S. (2017, 2017/11/02). Evidence that Recent Warming is Reducing Upper Colorado River Flows. *Earth Interactions*. doi: 10.1175/EI-D-17-0007.1

Milly, P. C. D., & Dunne, K. A. (2016, 10). Potential evapotranspiration and continental drying. *Nature Climate Change*, *6*(10), 946–949. doi: 10.1038/nclimate3046

Morice, C. P., Kennedy, J. J., Rayner, N. A., & Jones, P. D. (2012, 2020/02/26). Quantifying uncertainties in global and regional temperature change using an ensemble of observational estimates: The HadCRUT4 data set. *Journal of Geophysical Research: Atmospheres*, *117*(D8). Retrieved from `https://doi.org/10.1029/2011JD017187` doi: 10.1029/2011JD017187

Mote, P. W., Li, S., Lettenmaier, D. P., Xiao, M., & Engel, R. (2018). Dramatic declines in snowpack in the western US. *npj Climate and Atmospheric Science*, *1*(1), 2. doi: 10.1038/s41612-018-0012-1

Mote, P. W., Rupp, D. E., Li, S., Sharp, D. J., Otto, F., Uhe, P. F., … Allen, M. R. (2016). Perspectives on the causes of exceptionally low 2015 snowpack in the western United States. *Geophysical Research Letters*, n/a–n/a. doi: 10.1002/2016GL069965

Nasrollahi, N., AghaKouchak, A., Cheng, L., Damberg, L., Phillips, T. J., Miao, C., … Sorooshian, S. (2015, 2020/03/03). How well do CMIP5 climate simulations replicate historical trends and patterns of meteorological droughts? *Water Resources Research*, *51*(4), 2847–2864. Retrieved from https://doi.org/10.1002/2014WR016318 doi: 10.1002/2014WR016318

O'Neill, B. C., Tebaldi, C., van Vuuren, D. P., Eyring, V., Friedlingstein, P., Hurtt, G., ... Sanderson, B. M. (2016, 09). The Scenario Model Intercomparison Project (ScenarioMIP) for CMIP6. *Geoscientific Model Development*, *9*(9), 3461–3482. doi: 10.5194/gmd-9-3461-2016

Orlowsky, B., & Seneviratne, S. I. (2013). Elusive drought: uncertainty in observed trends and short- and long-term CMIP5 projections. *Hydrology and Earth System Sciences*, *17*(5), 1765–1781. Retrieved from https://www.hydrol-earth-syst-sci.net/17/1765/2013/ doi: 10.5194/hess-17-1765-2013

Otto, F. E. L., Wolski, P., Lehner, F., Tebaldi, C., van Oldenborgh, G. J., Hogesteeger, S., ... New, M. (2018, nov). Anthropogenic influence on the drivers of the Western Cape drought 2015–2017. *Environmental Research Letters*, *13*(12), 124010. Retrieved from https://doi.org/10.1088%2F1748-9326%2Faae9f9 doi: 10.1088/1748-9326/aae9f9

Padrón, R. S., Gudmundsson, L., & Seneviratne, S. I. (2019, 2020/03/03). Observational Constraints Reduce Likelihood of Extreme Changes in Multidecadal Land Water Availability. *Geophysical Research Letters*, *46*(2), 736–744. Retrieved from https://doi.org/10.1029/2018GL080521 doi: 10.1029/2018GL080521

Pendergrass, A. G. (2019). *Calculates ECS from CMIP6 using the Gregory Method.* Retrieved October 30, 2019, from https://github.com/apendergrass/cmip6-ecs doi: 10.5281/zenodo.3492165

Pendergrass, A. G., Knutti, R., Lehner, F., Deser, C., & Sanderson, B. M. (2017). Precipitation variability increases in a warmer climate. *Scientific Reports*, *7*(1), 17966. doi: 10.1038/s41598-017-17966-y

Seager, R., Hoerling, M., Schubert, S., Wang, H., Lyon, B., Kumar, A., ... Henderson, N. (2015, 2015/07/23). Causes of the 2011 to 2014 california drought. *Journal of Climate*. doi: 10.1175/JCLI-D-14-00860.1

Seager, R., Osborn, T. J., Kushnir, Y., Simpson, I. R., Nakamura, J., & Liu, H. (2019, 2019/11/04). Climate variability and change of mediterranean-type climates. *Journal of Climate*, *32*(10), 2887–2915. doi: 10.1175/JCLI-D-18-0472.1

Seferian, R. (2018). CNRM-CERFACS CNRM-ESM2-1 model output prepared for CMIP6 CMIP. Retrieved from https://doi.org/10.22033/ESGF/CMIP6.1391 doi: 10.22033/ESGF/CMIP6.1391

Seth, A., Rauscher, S. A., Biasutti, M., Giannini, A., Camargo, S. J., & Rojas, M. (2013, 2014/03/11). CMIP5 Projected Changes in the Annual Cycle of Precipitation in Monsoon Regions. *Journal of Climate*, *26*(19), 7328–7351. doi: 10.1175/JCLI-D-12-00726.1

Shi, H. X., & Wang, C. H. (2015). Projected 21st century changes in snow water equivalent over Northern Hemisphere landmasses from the CMIP5 model ensemble. *The Cryosphere*, *9*(5), 1943–1953. doi: 10.5194/tc-9-1943-2015

Swann, A. L. S. (2018). Plants and Drought in a Changing Climate. *Current Climate Change Reports*, *4*(2), 192–201. doi: 10.1007/s40641-018-0097-y

Swann, A. L. S., Hoffman, F. M., Koven, C. D., & Randerson, J. T. (2016). Plant responses to increasing CO2 reduce estimates of climate impacts on drought severity. *Proceedings of the National Academy of Sciences*, *113*(36), 10019-10024. doi: 10.1073/pnas.1604581113

Swart, N. C., Cole, J. N. S., Kharin, V. V., Lazare, M., Scinocca, J. F., Gillett, N. P., ... Sigmond, M. (2019). CCCma CanESM5 model output prepared for CMIP6 ScenarioMIP. Retrieved from https://doi.org/10.22033/ESGF/CMIP6.1317 doi: 10.22033/ESGF/CMIP6.1317

Tachiiri, K., Abe, M., Hajima, T., Arakawa, O., Suzuki, T., Komuro, Y., ... Kawamiya, M. (2019). MIROC MIROC-ES2L model output prepared for

CMIP6 ScenarioMIP. Retrieved from https://doi.org/10.22033/ESGF/CMIP6.936 doi: 10.22033/ESGF/CMIP6.936

Tatebe, H., & Watanabe, M. (2018). MIROC MIROC6 model output prepared for CMIP6 CMIP. Retrieved from https://doi.org/10.22033/ESGF/CMIP6.881 doi: 10.22033/ESGF/CMIP6.881

Taylor, K. E., Stouffer, R. J., & Meehl, G. A. (2012). An Overview Of CMIP5 And The Experiment Design. *Bulletin of the American Meteorological Society*, *93*(4), 485–498. doi: http://dx.doi.org/10.1175/BAMS-D-11-00094.1

Tierney, J. E., Ummenhofer, C. C., & deMenocal, P. B. (2015). Past and future rainfall in the horn of africa. *Science Advances*, *1*(9), e1500682. doi: 10.1126/sciadv.1500682

Ting, M., Seager, R., Li, C., Liu, H., & Henderson, N. (2018, 2018/08/30). Mechanism of Future Spring Drying in the Southwestern United States in CMIP5 Models. *Journal of Climate*, *31*(11), 4265–4279. doi: 10.1175/JCLI-D-17-0574.1

Trancoso, R., Larsen, J. R., McVicar, T. R., Phinn, S. R., & McAlpine, C. A. (2017). CO2-vegetation feedbacks and other climate changes implicated in reducing base flow. *Geophysical Research Letters*, *44*(5), 2310–2318. doi: doi:10.1002/2017GL072759

Trugman, A. T., Medvigy, D., Mankin, J. S., & Anderegg, W. R. L. (2018, 2019/05/13). Soil Moisture Stress as a Major Driver of Carbon Cycle Uncertainty. *Geophysical Research Letters*, *45*(13), 6495–6503. doi: 10.1029/2018GL078131

Ukkola, A. M., De Kauwe, M. G., Pitman, A. J., Best, M. J., Abramowitz, G., Haverd, V., ... Haughton, N. (2016). Land surface models systematically overestimate the intensity, duration and magnitude of seasonal-scale evaporative droughts. *Environmental Research Letters*, *11*(10), 104012. Retrieved from http://dx.doi.org/10.1088/1748-9326/11/10/104012 doi: 10.1088/1748-9326/11/10/104012

Ukkola, A. M., Pitman, A. J., De Kauwe, M. G., Abramowitz, G., Herger, N., Evans, J. P., & Decker, M. (2018, 2020/03/03). Evaluating CMIP5 Model Agreement for Multiple Drought Metrics. *Journal of Hydrometeorology*, *19*(6), 969–988. Retrieved from https://doi.org/10.1175/JHM-D-17-0099.1 doi: 10.1175/JHM-D-17-0099.1

Ukkola, A. M., Prentice, I. C., Keenan, T. F., van Dijk, A. I. J. M., Viney, N. R., Myneni, R. B., & Bi, J. (2016, 01). Reduced streamflow in water-stressed climates consistent with CO2 effects on vegetation. *Nature Climate Change*, *6*(1), 75–78. doi: doi:10.1038/nclimate2831

Vicente-Serrano, S. M., Quiring, S. M., Peña-Gallardo, M., Yuan, S., & Domínguez-Castro, F. (2019). A review of environmental droughts: Increased risk under global warming? *Earth-Science Reviews*, 102953. doi: https://doi.org/10.1016/j.earscirev.2019.102953

Voldoire, A. (2018). CNRM-CERFACS CNRM-CM6-1 model output prepared for CMIP6 CMIP. Retrieved from https://doi.org/10.22033/ESGF/CMIP6.1375 doi: 10.22033/ESGF/CMIP6.1375

Williams, A. P., Seager, R., Abatzoglou, J. T., Cook, B. I., Smerdon, J. E., & Cook, E. R. (2015). Contribution of anthropogenic warming to the 2012–2014 California drought. *Geophysical Research Letters*, *42*(16), 6819-6828. doi: 10.1002/2015GL064924

Wu, T., Chu, M., Dong, M., Fang, Y., Jie, W., Li, J., ... Zhang, Y. (2018). BCC BCC-CSM2MR model output prepared for CMIP6 CMIP historical. Retrieved from https://doi.org/10.22033/ESGF/CMIP6.2948 doi: 10.22033/ESGF/CMIP6.2948

Xiao, M., Udall, B., & Lettenmaier, D. P. (2018). On the Causes of Declining Colorado River Streamflows. *Water Resources Research*, *54*(9), 6739–6756. doi:

doi:10.1029/2018WR023153

Yukimoto, S., Koshiro, T., Kawai, H., Oshima, N., Yoshida, K., Urakawa, S., ... Adachi, Y. (2019). MRI MRI-ESM2.0 model output prepared for CMIP6 CMIP. Retrieved from https://doi.org/10.22033/ESGF/CMIP6.621 doi: 10.22033/ESGF/CMIP6.621

Zhang, B., & Soden, B. J. (2019, 2020/03/03). Constraining Climate Model Projections of Regional Precipitation Change. *Geophysical Research Letters*, *46*(17-18), 10522–10531. Retrieved from https://doi.org/10.1029/2019GL083926 doi: 10.1029/2019GL083926

Zhang, X., Tang, Q., Zhang, X., & Lettenmaier, D. P. (2014, 2019/11/12). Runoff sensitivity to global mean temperature change in the CMIP5 Models. *Geophysical Research Letters*, *41*(15), 5492–5498. doi: 10.1002/2014GL060382

Zhang, Y., Peña-Arancibia, J. L., McVicar, T. R., Chiew, F. H. S., Vaze, J., Liu, C., ... Pan, M. (2016). Multi-decadal trends in global terrestrial evapotranspiration and its components. *Scientific Reports*, *6*(1), 19124. Retrieved from https://doi.org/10.1038/srep19124 doi: 10.1038/srep19124

Zhou, S., Williams, A. P., Berg, A. M., Cook, B. I., Zhang, Y., Hagemann, S., ... Gentine, P. (2019, 09). Land–atmosphere feedbacks exacerbate concurrent soil drought and atmospheric aridity. *Proceedings of the National Academy of Sciences*, *116*(38), 18848. Retrieved from http://www.pnas.org/content/116/38/18848.abstract doi: 10.1073/pnas.1904955116

Figure 1.

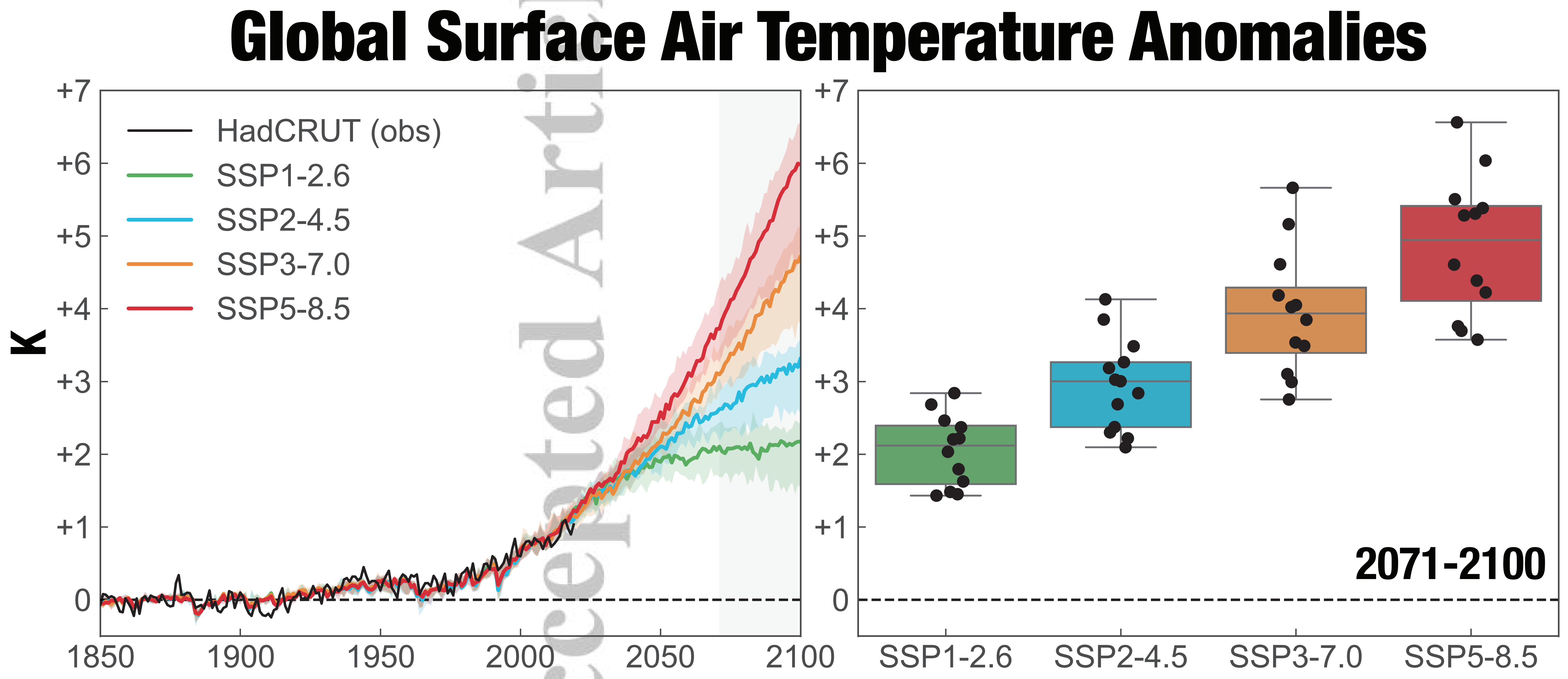
Global Surface Air Temperature Anomalies
K
+7
+6
+5
+4
+3
+2
+1
0
HadCRUT (obs)
SSP1-2.6
SSP2-4.5
SSP3-7.0
SSP5-8.5
1850
1900
1950
2000
2050
2100
2071-2100
SSP1-2.6
SSP2-4.5
SSP3-7.0
SSP5-8.5

Figure 2.

SSP1-2.6
SSP2-4.5
SSP3-7.0
DJF
MAM
JJA
SON
−60
−40
−20
0
20
40
60
%
ΔPrecipitation

Figure 3.

SSP1-2.6
SSP2-4.5
SSP3-7.0
ΔSoil Moisture
(surface)
ONDJFM
AMJJAS
ΔSoil Moisture
(column)
ONDJFM
AMJJAS
z-score
−5
−4
−3
−2
−1
0
1
2
3
4
5

Figure 4.


SSP1-2.6
SSP2-4.5
SSP3-7.0
ΔRunoff
(surface)
ΔRunoff
(total)
ONDJFM
AMJJAS
%
−60
−40
−20
0
20
40
60

Figure 5.

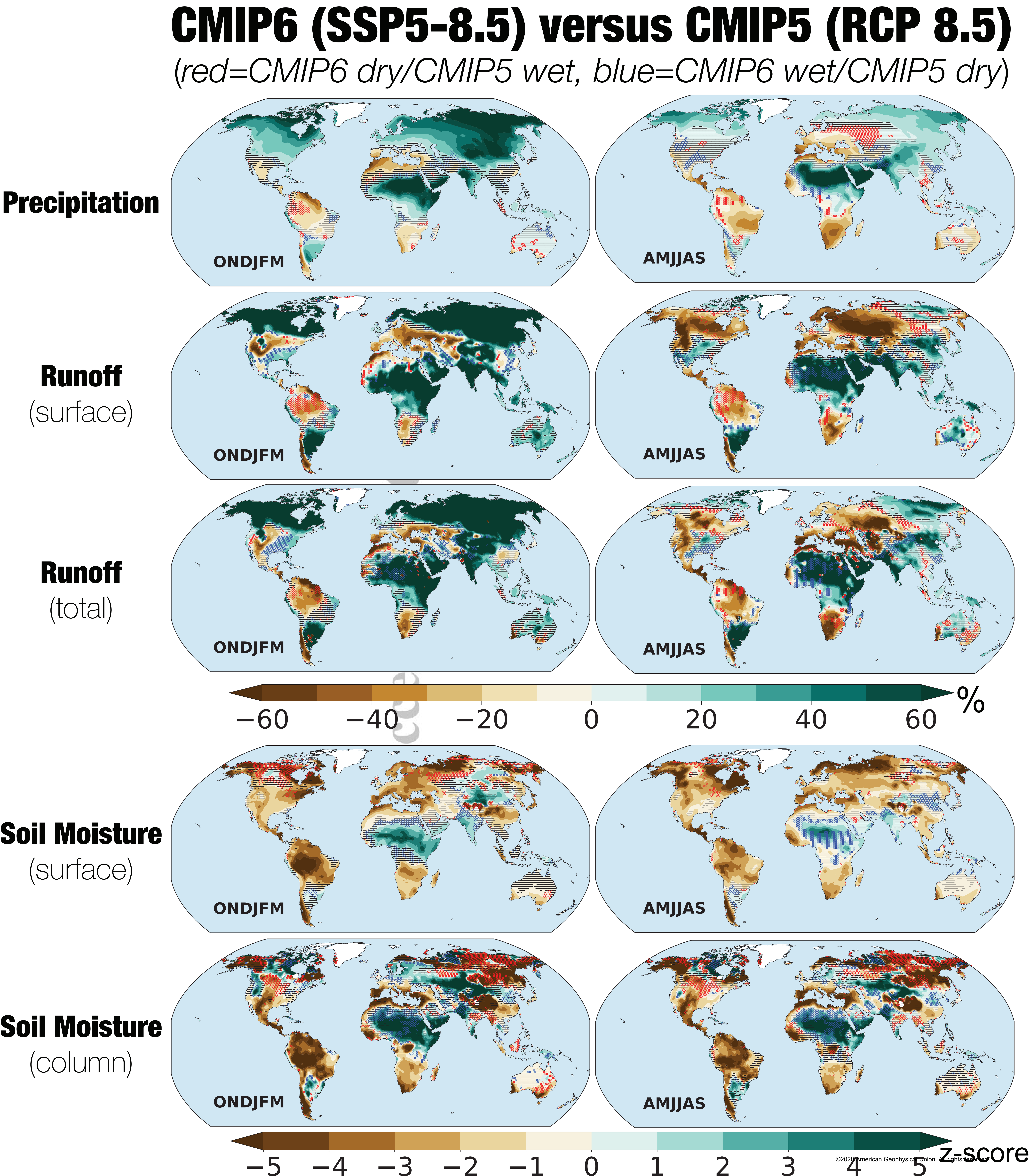
CMIP6 (SSP5-8.5) versus CMIP5 (RCP 8.5)
(red=CMIP6 dry/CMIP5 wet, blue=CMIP6 wet/CMIP5 dry)
Precipitation
Runoff
(surface)
Runoff
(total)
Soil Moisture
(surface)
Soil Moisture
(column)
ONDJFM
AMJJAS
−60
−40
−20
0
20
40
60
%
−5
−4
−3
−2
−1
0
1
2
3
4
5
z-score
©2020 American Geophysical Union. All rights reserved.

Figure 6.

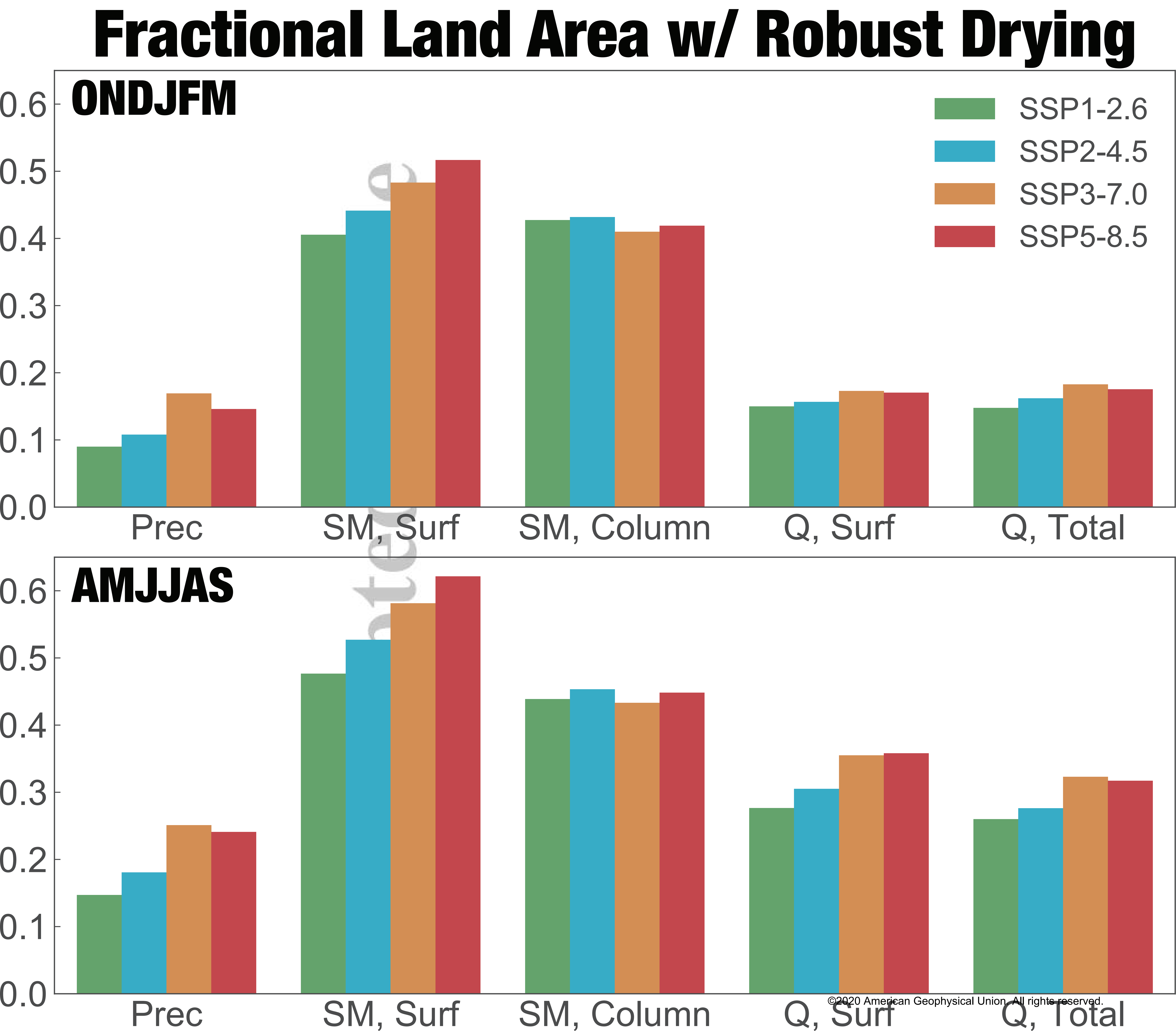

Fractional Land Area w/ Robust Drying
ONDJFM
AMJJAS
SSP1-2.6
SSP2-4.5
SSP3-7.0
SSP5-8.5
0.0
0.1
0.2
0.3
0.4
0.5
0.6
Prec
SM, Surf
SM, Column
Q, Surf
Q, Total

Figure 7.

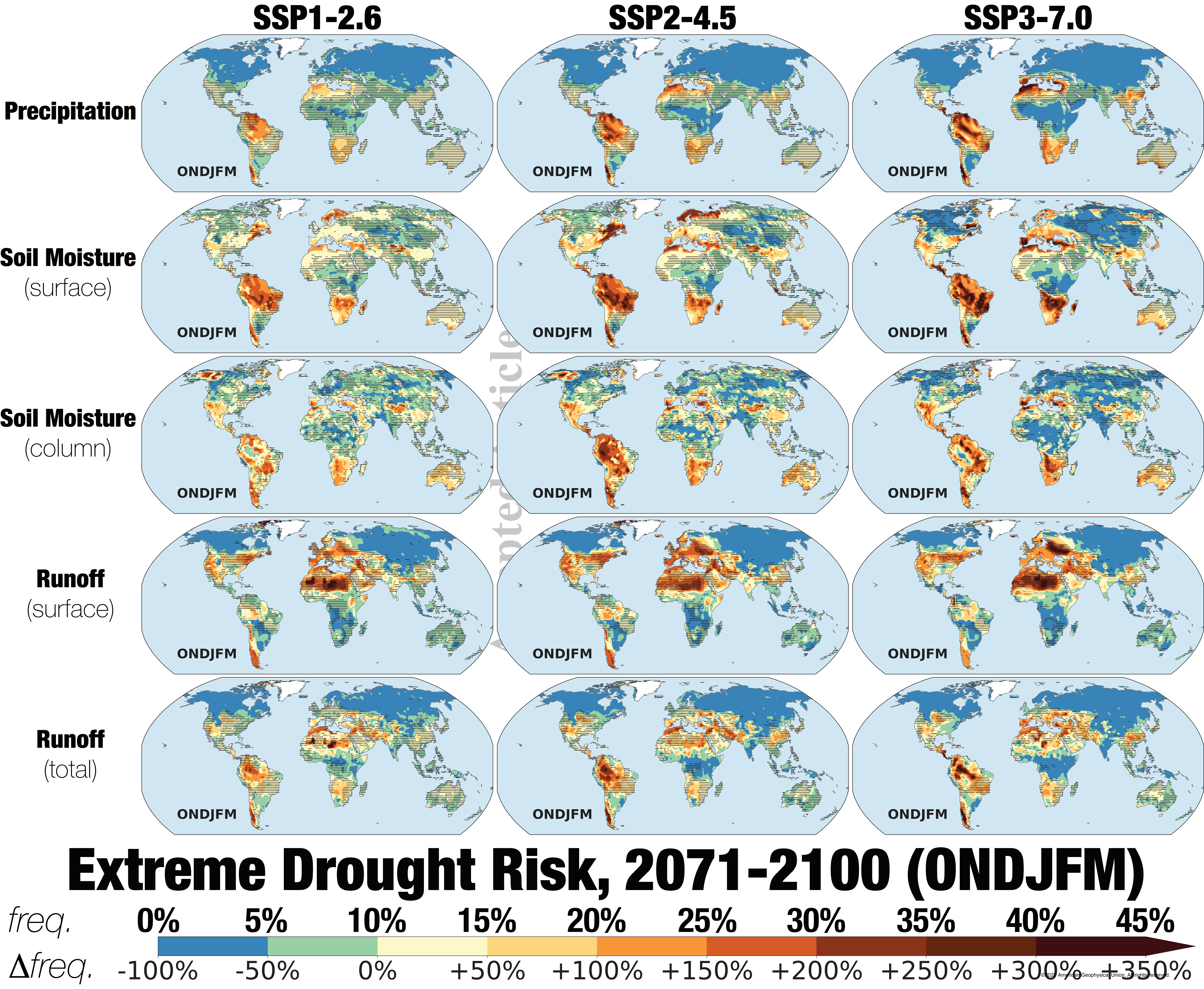

SSP1-2.6
SSP2-4.5
SSP3-7.0
Precipitation
Soil Moisture
(surface)
Soil Moisture
(column)
Runoff
(surface)
Runoff
(total)
ONDJFM
Extreme Drought Risk, 2071-2100 (ONDJFM)
freq.
0%
5%
10%
15%
20%
25%
30%
35%
40%
45%
Δfreq.
-100%
-50%
0%
+50%
+100%
+150%
+200%
+250%
+300%
+350%

Figure 8.

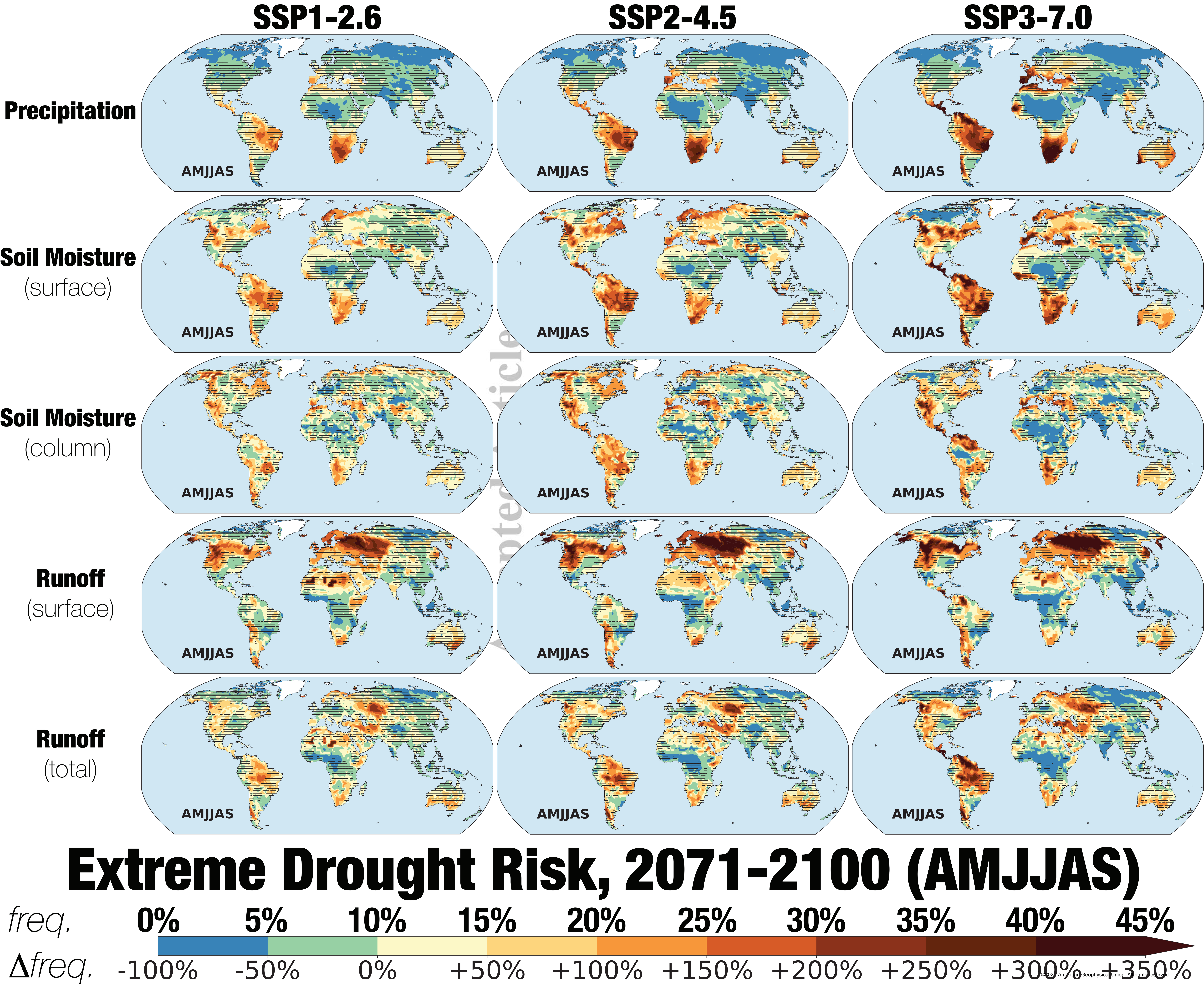
SSP1-2.6
SSP2-4.5
SSP3-7.0
Precipitation
Soil Moisture (surface)
Soil Moisture (column)
Runoff (surface)
Runoff (total)
AMJJAS
Extreme Drought Risk, 2071-2100 (AMJJAS)
freq.
0% 5% 10% 15% 20% 25% 30% 35% 40% 45%
Δfreq.
-100% -50% 0% +50% +100% +150% +200% +250% +300% +350%

Figure 9.

ΔPrecipitation
ΔRunoff (surface)
ΔRunoff (total)
SSP1-2.6
SSP2-4.5
SSP3-7.0
SSP5-8.5
ANNUAL
−60
−40
−20
0
20
40
60
%
Changes in Drought (annual, 1851-1880 baseline)

Figure 10.

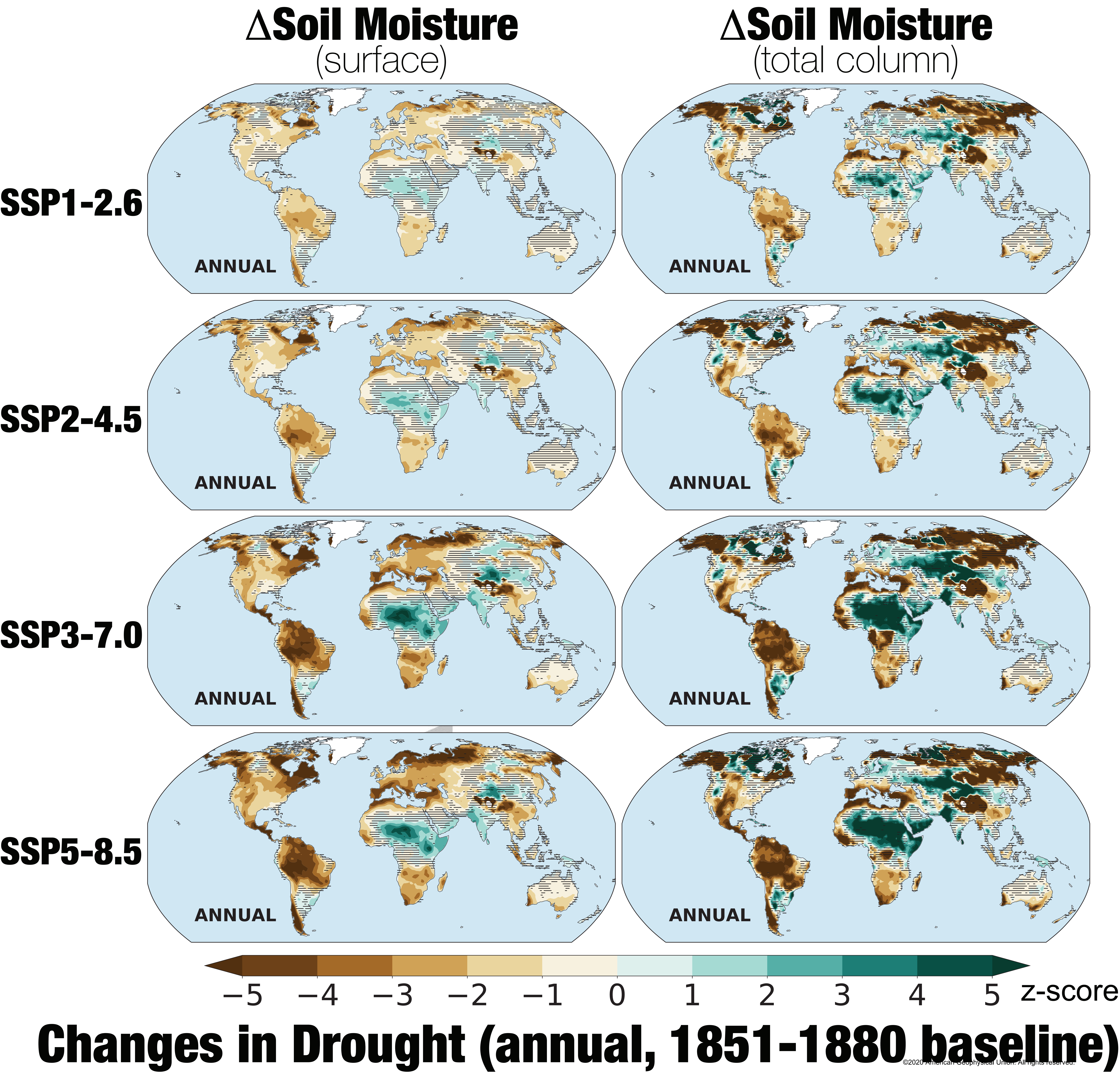

ΔSoil Moisture
(surface)
ΔSoil Moisture
(total column)
SSP1-2.6
SSP2-4.5
SSP3-7.0
SSP5-8.5
ANNUAL
−5
−4
−3
−2
−1
0
1
2
3
4
5
z-score
Changes in Drought (annual, 1851-1880 baseline)

Figure 11.


ΔPrecipitation
ΔRunoff
(surface)
ΔRunoff
(total)
SSP1-2.6
SSP2-4.5
SSP3-7.0
SSP5-8.5
ANNUAL
−60
−40
−20
0
20
40
60
%
Changes in Drought (annual, 1985-2014 baseline)

Figure 12.

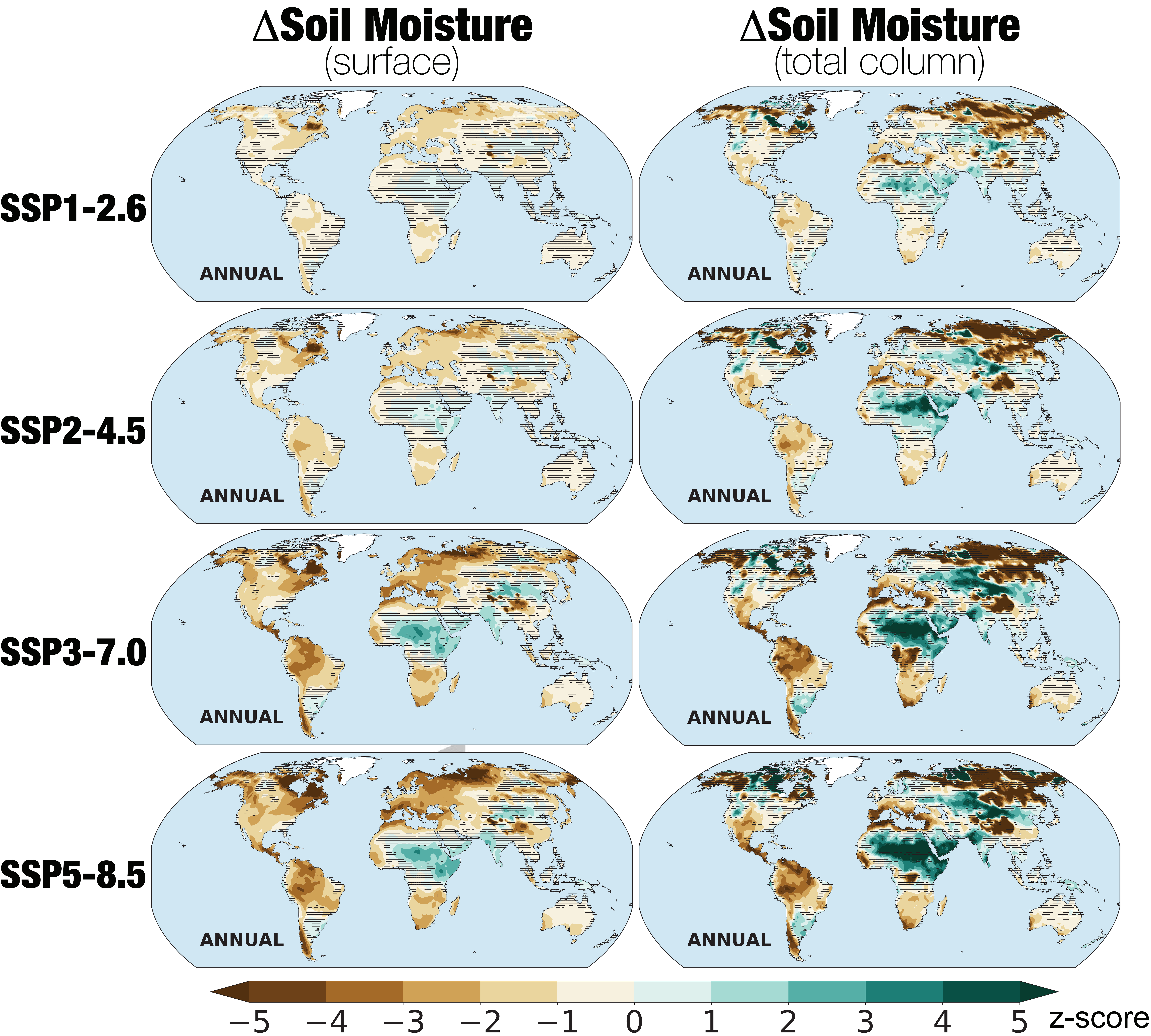

Changes in Drought (annual, 1985-2014 baseline)